JCTC Journal of Chemical Theory and Computation

Perspective

pubs.acs.org/JCTC

# Excitation Gaps of Finite-Sized Systems from Optimally Tuned Range-Separated Hybrid Functionals

Leeor Kronik,*[,†] Tamar Stein,[‡] Sivan Refaely-Abramson,[†] and Roi Baer*[,‡]

[†]Department of Materials and Interfaces, Weizmann Institute of Science, Rehovoth 76100, Israel

[‡]Fritz Haber Center for Molecular Dynamics, Institute of Chemistry, Hebrew University, Jerusalem 91904 Israel

**ABSTRACT:** Excitation gaps are of considerable significance in electronic structure theory. Two different gaps are of particular interest. The fundamental gap is defined by charged excitations, as the difference between the first ionization potential and the first electron affinity. The optical gap is defined by a neutral excitation, as the difference between the energies of the lowest dipole-allowed excited state and the ground state. Within many-body perturbation theory, the fundamental gap is the difference between the corresponding lowest quasi-hole and quasi-electron excitation energies, and the optical gap is addressed by including the interaction between a quasi-electron and a quasi-hole. A long-standing challenge has been the attainment of a similar description within density functional theory (DFT), with much debate on whether this is an achievable goal even in principle. Recently, we have constructed and applied a new approach to this problem. Anchored in the rigorous theoretical framework of the generalized Kohn−Sham equation, our method is based on a range-split hybrid functional that uses exact long-range exchange. Its main novel feature is that the range-splitting parameter is not a universal constant but rather is determined from first principles, per system, based on satisfaction of the ionization potential theorem. For finite-sized objects, this DFT approach mimics successfully, to the best of our knowledge for the first time, the quasi-particle picture of many-body theory. Specifically, it allows for the extraction of both the fundamental and the optical gap from one underlying functional, based on the HOMO−LUMO gap of a ground-state DFT calculation and the lowest excitation energy of a linear-response time-dependent DFT calculation, respectively. In particular, it produces the correct optical gap for the difficult case of charge-transfer and charge-transfer-like scenarios, where conventional functionals are known to fail. In this perspective, we overview the formal and practical challenges associated with gap calculations, explain our new approach and how it overcomes previous difficulties, and survey its application to a variety of systems.

## INTRODUCTION

Of particular significance in spectroscopy are excitation gaps. Two different gaps are of both theoretical and practical importance.[1,2] The *fundamental gap*, $E_g$, is defined by charged excitations as the difference between the first ionization potential, $I$, and the first electron affinity, $A$. The *optical gap*, $E_{opt}$, is defined by a neutral excitation, as the difference between the energies of the lowest dipole-allowed excited state and the ground state. Both are accessible experimentally, but in different ways. The fundamental gap can be determined as the difference of two observables, $I$ and $A$, e.g., by using photoemission and inverse photoemission, respectively, or tunneling spectroscopy involving electron removal or injection, respectively. The optical gap can be measured, for example, by determining the onset of the absorption spectrum.

The relation between the two gaps can be understood intuitively by considering the concept of a quasi-particle.[3] As an electron is inserted, or ejected (leaving a hole behind), all other electrons in the system respond to the presence of this extra electron or hole. The single particle picture can be retained, however, by thinking of *quasi*-electrons or *quasi*-holes, respectively, i.e., of effective particles that contain ("are dressed by") the effects of the relaxation of the other electrons. The ionization potential and electron affinity are, then, the lowest quasi-hole and quasi-electron excitation energies, respectively (Figure 1a).

Creation of an excited state by promoting an electron can then be considered as the simultaneous creation of a quasi-particle and a quasi-hole (Figure 1b). If these two quasi-particles are noninteracting, the minimum energy for such excitation will be given by the fundamental gap. In practice, however, clearly they do interact. The optical gap therefore differs from the fundamental gap by the interaction energy between the quasi-particles. We refer to this energy as the exciton (i.e., quasi-electron−quasi-hole pair) binding energy, $E_B$.

Further insight into the difference and relation between the two gaps is obtained by considering a special limiting case—that of a donor (D)−acceptor (A) complex, where the chemical interaction between the donor and acceptor molecules can be neglected. For this limit, Mulliken has determined that the lowest excitation which transfers charge from donor to acceptor, $h\nu_{CT}$, would be given (in atomic units) by[4]

$$h\nu_{CT} = I_D - A_A - 1/R \quad (1)$$

where $R$ is the donor−acceptor distance. Here, the difference $I_D - A_A$ is the fundamental gap *of the entire complex*, which is dictated by the ionization potential of the donor and the electron affinity of the acceptor. If the intramolecular excitation energies are such that $h\nu_{CT}$ is the lowest optical excitation energy (which is often the case in charge-transfer-excitation

Received: December 30, 2011
Published: March 19, 2012

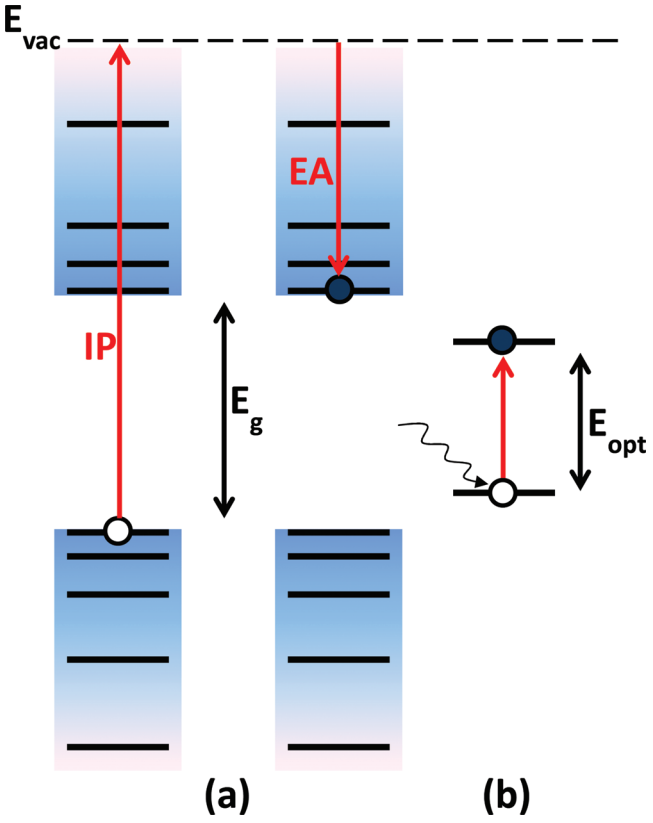


**Figure 1.** (a) Schematic representation of the lowest-energy excitation of a quasi-hole (left) or a quasi-electron (right), corresponding to the ionization potential (IP) or the electron affinity (EA), respectively, the difference of which is the fundamental gap, $E_g$. (b) Schematic representation of the lowest-energy excitation of both a quasi-electron and a quasi-hole, corresponding to the optical gap, $E_{opt}$. In the drawing, $E_{vac}$ is the vacuum level, and $E_{opt}$ is smaller than $E_g$ by the attraction energy between the quasi-electron and the quasi-hole.

complexes), then $h\nu_{CT}$ is the optical gap, and it is smaller than the fundamental gap precisely by the binding energy $1/R$ between the quasi-electron placed on the acceptor and the quasi-hole left behind on the donor.

Computing the two gaps from first principles, i.e., without recourse to any empirically derived information, is difficult. These can obviously be derived from wave-function-based *ab initio* methods (see, e.g., refs 5−10) or from quantum Monte Carlo methods (see, e.g, refs 11−13), but the computational cost is very high, limiting practical calculations to small systems, and the intuition afforded by the quasi-particle picture is lost.

The qualitative quasi-particle picture can be translated into formal language using many-body perturbation theory.[14] Quasi-particle energies and orbitals, leading to the fundamental gap, can then be determined directly as eigenvalues and eigenfunctions of the Dyson equation[15] (typically solved within the GW approximation,[1,16−18] where $G$ is the Green function and $W$ is the screened Coulomb potential). Optical excitation energies, the lowest allowed of which is $E_{opt}$, can then be determined from the Bethe−Salpeter equation (BSE).[1,14,19,20] While the GW-BSE approach is well-grounded theoretically and often highly reliable in practice, the computational cost associated with it for large systems is still too high for many important applications (see, e.g., ref 21 and references therein).

A different method based on single-particle energies and orbitals is density functional theory (DFT),[22,23] discussed in more detail below. In recent years, DFT has become the method of choice for electronic-structure calculations across an unusually wide variety of disciplines,[24] from organic chemistry[25] to condensed matter physics,[26] as it allows for fully quantum-mechanical calculations at a relatively modest computational cost. Ideally, one would have liked to compute the fundamental gap from the energy difference between the highest occupied molecular orbital (HOMO) and the lowest unoccupied molecular orbital (LUMO) energies of a DFT calculation. However, this is considered to be unjustified theoretically in principle (an issue we return to in detail below)[27,28] and indeed often yields results in very poor agreement with fundamental gaps in practice.[2] For finite-sized objects, the fundamental gap can always be computed, at least in principle, from the total energies of the neutral, cation, and anion. But the eigenvalues are needed for, e.g., conductance calculations based on DFT (where reliance on approximate values can lead to gross errors[29−31]). Furthermore, one would prefer to retain, inasmuch as this is possible, an intuitive connection between single-particle energy levels and particle excitations.

Optical excitations, on the other hand, *can* be computed from a time-dependent DFT (TDDFT) calculation.[32−34] The approach is rigorous in principle and often successful in practice. However, certain types of optical excitations, notably charge-transfer excitations, a limiting case of which has been discussed above, typically defy proper description using conventional approximations employed in TDDFT calculations.[35,36]

An outstanding question, then, is whether the quasi-particle picture of the fundamental and optical gap can be restored to (TD)DFT, at least to a degree of approximation useful for quantitative comparison with experimental results. In this article, we show that this is indeed possible, using a new concept, elaborated below, of the optimally tuned range-separated hybrid functional. We show that, for a finite system, this approach resolves the long-standing fundamental gap question within DFT and allows for quantitative prediction of the optical gap within TDDFT, even for full or partial charge transfer or charge-transfer-like scenarios.

## FUNDAMENTAL GAPS FROM KOHN−SHAM THEORY?

The central tenet of DFT is the Hohenberg−Kohn theorem,[37] which states that the ground-state density, $n(r)$, of a system of interacting electrons in some external potential, $v_{ext}(r)$, determines this potential uniquely (up to an uninteresting additive constant). In the Kohn−Sham (KS) approach to DFT,[38] the Hohenberg−Kohn theorem is utilized to show that the ground state of the physical interacting-electron system can be mapped into the ground state of an equivalent system of fictitious noninteracting electrons that are subject to a common *local* (i.e., multiplicative) external potential, in the form

$$\left(-\frac{\nabla^2}{2} + v_{ext}(r) + v_H([n]; r) + v_{xc}([n]; r)\right)\varphi_i(r) = \varepsilon_i\varphi_i(r) \quad (2)$$

where $v_{ext}(r)$ is the ion-electron potential, $v_H([n];r)$ is the Hartree potential, which accounts for the classical electron−electron Coulomb repulsion, $v_{xc}([n];r)$ is the exchange-correlation (xc) potential, which accounts for all nonclassical electron interactions, and $\varepsilon_i$ and $\varphi_i(r)$ are KS eigenvalues and


dx.doi.org/10.1021/ct2009363 | J. Chem. Theory Comput. 2012, 8, 1515−1531

orbitals, respectively. The electron density is calculated as a sum over filled orbitals:

$$n(r) = \sum_{i,\mathrm{occ}} |\varphi_i(r)|^2 \tag{3}$$

Atomic units are used throughout, and for simplicity only the spin-unpolarized formalism is given. The KS mapping is exact, in the sense that the self-consistent electron density determined from eqs 1 and 2 should be equal to that of the physical system. In practice, however, only approximate forms for $v_{xc}([n];r)$ are available.

Even if the exact $v_{xc}([n];r)$ were known, the physical interpretation of KS eigenvalues and orbitals as single-particle quantities is still far from straightforward. Strictly speaking, the KS system is fictitious, and the KS quantities can be viewed as mere mathematical devices en route to obtaining the correct ground-state density. Some approximate relations between KS and quasi-particle eigen-pairs do exist,[39,40] but because here we are interested only in the fundamental gap, we focus our attention first on the KS HOMO.

Exact physical meaning can be assigned to the KS HOMO using "the KS analogue of Koopmans' theorem in Hartree–Fock theory",[41−44] which states that for the exact theory, the KS HOMO is equal to and opposite of the ionization potential, i.e.,

$$\varepsilon_H = -I \tag{4}$$

The KS version of Koopmans' theorem is in fact stronger than the original, Hartree–Fock-based one.[45] In Hartree–Fock theory, a relation similar to eq 4 is valid only for *unrelaxed* electron removal (i.e., neglecting the response of the other electrons in the system). In KS theory, relaxation effects are included in eq 4, and $\varepsilon_{HOMO}$ is rigorously the lowest quasi-hole excitation energy, which is precisely the kind of intuition we were looking for.

One way to rationalize eq 4[42,44] is to consider that in the interacting electron system the electron density decays asymptotically as $n(r) \approx e^{-2(2I)^{1/2}r}$. For the KS system, the density is the same but is expressed as a sum of orbital densities $|\varphi_i(r)|^2$ (eq 3). Each such term decays asymptotically as $|\varphi_i(r)|^2 \approx e^{-2(-2\varepsilon_i r)^{1/2}}$, and the asymptotic behavior will ultimately be dominated by the KS HOMO, whose decay is slowest. Comparing the two decay expressions, the real and KS densities can only be reconciled if eq 4 is obeyed.

Can one equally well prove a second Koopmans' theorem, that would identify the KS LUMO with the lowest quasi-electron excitation energy, $A$? Unfortunately, the answer is a resounding no.[27,28] To understand why, we digress briefly to the generalization of the ground state energy to systems with a fractional number of electrons, which is needed for the description of open systems.[22,41] The argument proceeds by considering an ensemble (statistical mixture) of $M$ and $M + 1$ pure-state electron densities, yielding the desired fractional one. Minimization of the energy with respect to number-conserving variations of the ensemble electron density then shows that the minimum energy is simply a linear combination of the pure-state energies, based on the relative fraction of their densities in the ensemble density.[41] Therefore, for any system, the exact total energy versus particle number curve must be a series of linear segments, as shown in Figure 2 (left).

The slopes of $(N - 1, N)$ and $(N, N + 1)$ segments are, by definition, $-I$ and $-A$, respectively; i.e., the derivative of the total energy with respect to particle number is discontinuous at the $N$-electron point. This is physically reasonable—it is simply a reflection of the discontinuity in the chemical potential, i.e., the fact that the electron removal energy is not the same as the electron insertion energy (namely, that the fundamental gap is nonzero). Now consider what happens in the KS descriptions of these segments. Because the energy contributions of the external potential and the Hartree potential are continuous with respect to the density, such discontinuity can arise, in principle, from either the kinetic energy of the noninteracting electrons or from the xc energy. A discontinuity in the latter would correspond to a (spatially constant[46]) discontinuity in $v_{xc}([n];r)$ at an integer particle number, usually known as a derivative discontinuity (DD), $\Delta_{xc}$.[41] While in some cases $\Delta_{xc}$ can be small (i.e., the discontinuity in the chemical potential is mostly described by the kinetic energy term),[47] both formal considerations[27,28] and numerical investigation[48] show that it is usually sizable. For example, reconstruction of the exact exchange-correlation potential from the charge density obtained from wave-function-based quantum chemistry calculations yields derivative discontinuities that are easily several eV.[49,50]

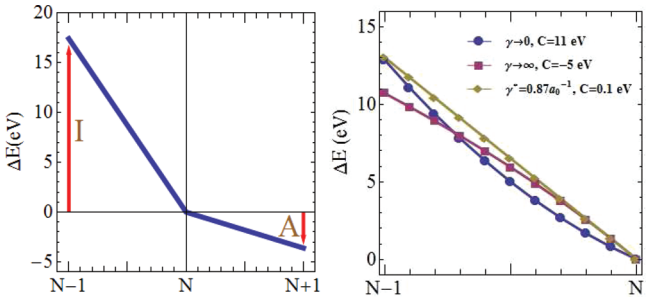


**Figure 2.** Left: The "linear segment" behavior of the exact density functional (the numerical values are the experimental ones for the F atom, as an example) − the total energy (with respect to that of the $N$ electron neutral species), $\Delta E$, is a series of linear segments. The slopes of the $[N - 1, N]$ and the $[N, N + 1]$ segments correspond to the ionization potential, $I$, and electron affinity, $A$, respectively. Right: DFT total energy difference with respect to the neutral, $N = 10$ electron system, $\Delta E$, as a function of the particle number $N$ for the $H_2O$ molecule, calculated with the Baer–Neuhauser (BN) functional with $\gamma \to 0$, $\gamma \to \infty$, and the optimally tuned $\gamma^* = 0.87$. The average curvature, $C = d^2E/dN^2$, is indicated for each functional. Figure adapted from Stein et al.[175]

Now, a different condition which must be obeyed in KS theory is Janak's theorem, which asserts that each occupied eigenvalue is given by the derivative of the energy with respect to the occupation of this orbital.[51] Applying this rule to the KS HOMO, the derivative is by construction the above-mentioned slope of the piecewise-linear curve of Figure 2 (left). But this slope can be either $-I$ or $-A$ at the integer particle number! Therefore, eq 4 is obeyed only if the integer particle number is approached from below. Fortunately, this "direction of approach to the integer point" is the one obtained automatically by assuming the KS potential (= sum of all potentials in eq 2) to be zero at infinity,[44] which is usually the default choice.

The above arguments regarding the asymptotic decay of the density are inapplicable to the KS LUMO because it is unoccupied. However, ignoring nuclear relaxation effects, the electron affinity of the $N$ electron system is equal to the ionization potential of the $N + 1$ electron one, so that by application of eq 4 to the $N + 1$ electron system we obtain $\varepsilon_H(N + 1 - \delta) = -A$, where $\delta$ is a positive infinitesimal that guarantees that we approach the integer point from below. But because of the straight-line dependence, the slope just to the left of the $N + 1$ electron point is the same as the slope just to the right of the $N$ electron point, and therefore $\varepsilon_H(N + 1 - \delta) = \varepsilon_H(N + \delta)$. In addition, $\varepsilon_H(N + \delta) = \varepsilon_L(N - \delta) + \Delta_{xc}$ because the


dx.doi.org/10.1021/ct2009363 | J. Chem. Theory Comput. 2012, 8, 1515−1531

xc potential "jumps" by $\Delta_{xc}$ as we cross the integer point (note that the HOMO for $N + \delta$ electrons is the LUMO for $N - \delta$ electrons). This immediately leads to a regrettable result:[52]

$$\varepsilon_L = -A - \Delta_{xc} \quad (5)$$

where we have suppressed the infinitesimal $\delta$ to emphasize that eq 5 is what we expect to obtain when eq 4 is obeyed. In other words, even in exact KS theory, if the asymptotic potential is chosen such that KS HOMO reflects the lowest quasi-hole excitation energy, the KS LUMO will not reflect the lowest quasi-electron excitation energy! Furthermore, by combining eqs 4 and 5 we obtain:[28]

$$E_g \equiv I - A = \varepsilon_L - \varepsilon_H + \Delta_{xc} \quad (6)$$

We find, therefore, that the KS framework is inherently incompatible with a simultaneous interpretation of $\varepsilon_{HOMO}$ and $\varepsilon_{LUMO}$ as quasi-particle levels, and comparison of KS gaps to fundamental ones is inherently a comparison of apples and oranges.[2]

So far, we only discussed properties of the exact, but unknown, KS mapping. The two most common practical approximate mappings are the local density approximation (LDA) and the generalized gradient approximation (GGA).[22,23] In LDA, we assume that the xc energy per particle at each point in space is given by its value for the uniform electron gas. This makes $v_{xc}([n];r)$ a simple function (rather than a functional) of $n(r)$. In GGA, some account of nonuniformity is achieved by considering $v_{xc}([n];r)$ as a function of the electron density as well as its gradient. Given the explicit density dependence, neither LDA nor GGA can exhibit any DD. Instead, they approximately average over the DD.[28,53] Therefore, even when LDA or GGA act as good approximations for ground state properties, they underestimate $I$ and overestimate $A$ by $\sim\Delta_{xc}/2$,[54] such that neither is exact.

We emphasize that because the KS framework is exact, one can still extract fundamental gaps from other considerations. For example, for finite systems, one can always compute the fundamental gap from differences of ground state energies (for the anion, cation, and neutral),[23] with a generalization to the solid state recently suggested.[55] Other recent ideas include a scissors-like operator based on the difference between the $N + 1$ and $N$-particle Hamiltonians[30,56] or the assessment of the derivative discontinuity from a correction scheme that is based on fixing the asymptotic behavior of an approximate exchange-correlation potential.[57] However, these approaches do not allow for the identification of the lowest quasi-particle excitation energies with $\varepsilon_{HOMO}$ and $\varepsilon_{LUMO}$ that arise simultaneously from one self-consistent single-particle Hamiltonian corresponding to $N$ electrons. Therefore, we must seek further answers outside the KS framework.

## FUNDAMENTAL GAPS FROM GENERALIZED KOHN–SHAM THEORY

In their pioneering 1965 article,[38] Kohn and Sham also briefly discussed the possibility of a scheme that would map the original system into a Hartree–Fock system having the same density, which is obviously subject to a *nonlocal* (i.e., nonmultiplicative) exchange potential. Nevertheless, a rigorous basis for such a mapping did not emerge until more than 30 years later. In their seminal 1996 article,[58] Seidl et al. pointed out that the original KS scheme involved mapping into a system that, by virtue of its noninteracting-particle nature, could be described by a single Slater determinant. However, one could equally well attempt to rely on the Hohenberg–Kohn theorem to map the real system into any *interacting* model system that can still be represented by a single Slater determinant but will no longer necessarily be described by a strictly local potential. They proved that such an alternate mapping can be achieved in practice by defining an energy functional, $S[\{\varphi_i\}]$, of the orbitals $\{\varphi_i\}$ comprising the Slater determinant of the model system and expressing the total energy as a sum of $S[\{\varphi_i\}]$, the ion-electron attraction, and a "remainder" term. One next seeks the Slater determinant that minimizes this form of the energy functional while yielding the density of the original system via eq 3. The minimizing orbitals then play a role analogous to that of the KS orbitals. This procedure leads to a *generalized* Kohn–Sham (GKS) equation, in the form

$$(\hat{O}_s[\{\varphi_i\}] + v_{ext}(r) + v_R([n];r))\varphi_j(r) = \varepsilon_j\varphi_j(r) \quad (7)$$

where $\hat{O}_s[\{\varphi_i\}]$ is a generally *nonlocal*, orbital-specific operator, and $v_R([n];r)$ is a "remainder" local potential, which is a functional of the density, and which is determined from a functional derivative of the "remainder" energy term.

Formally, both the KS and the GKS maps are exact.[58] But whereas there is only one KS map, there exist a multitude of GKS maps, depending on the choice of $S[\{\varphi_i\}]$. Two special GKS maps help in clarifying the physical similarities and differences between the KS and GKS maps.[58] If one chooses $S[\{\varphi_i\}]$ to be the kinetic energy of the fictitious system, then $\hat{O}_s[\{\varphi_i\}]$ is simply the usual single-particle kinetic energy operator, i.e., the first term in the KS equation. The "remainder" potential $v_R([n];r)$ is then simply the sum of the Hartree and exchange-correlation terms of the KS equation, and the KS and GKS equations are one and the same. However, if one chooses $S[\{\varphi_i\}]$ to be the Slater-determinant expectation value of the sum of the kinetic energy and electron-repulsion energy operators, then $\hat{O}_s[\{\varphi_i\}]$ is the sum of the single-particle kinetic energy operator and the Hartree–Fock operator, and the "remainder" potential $v_R([n];r)$ is then a correlation potential. This "Hartree–Fock–Kohn–Sham" equation is then also a special case of a GKS map. Unlike the original Hartree–Fock equation, the "Hartree–Fock–Kohn–Sham" equation is in principle exact. In practice, of course, little is known about the exact $v_R([n];r)$. But we do know that it is different from the KS correlation potential, because the *local* exact exchange potential in the KS scheme is different from the *nonlocal* exact (Fock) operator in the GKS scheme.[2]

Other choices for GKS maps, which allow for practical approximations, are considered below. But first, let us discuss what one can and cannot expect from exact GKS calculations. Naively, one would think that because GKS electrons are partially interacting, interpretation of charged excitations in terms of single-electron energy levels would, if anything, become more difficult. Indeed, little is known about general properties of the GKS equation for a completely arbitrary $S[\{\varphi_i\}]$ (and ensuing $\hat{O}_s[\{\varphi_i\}]$).

Fortunately, for the specific yet important case of a Fock (exact-exchange) nonlocal operator, it is still possible to identify the GKS HOMO energy with $-I$.[59] One way to rationalize this is that with Hartree–Fock–Kohn–Sham electrons, unlike with KS electrons, the asymptotic decay of *all* orbitals is (generally) dictated by the highest occupied eigenvalue, as $|\varphi_i(r)|^2 \approx e^{-2(-2\varepsilon_H r)^{1/2}}$.[60] But because the Hartree–Fock density is still given by eq 3, and because the original density still decays asymptotically as $n(r) \approx e^{-2(2I)^{1/2}r}$, it follows that the real and Hartree–Fock densities can only be reconciled if eq 4 is still obeyed. In this sense, then, the exact Fock-based GKS mapping is equivalent to the KS one.[61]

What about the GKS result that would be analogous to eq 5? Recall that for the KS map, the exchange-correlation potential had to "absorb" whatever discontinuity of the chemical potential that was not reflected in the kinetic energy term. In the GKS equation, some of this "burden" can be shouldered by the other nonlocal terms, e.g., the Fock one. Thus, it can be expected quite generally that the DD in the "remainder" potential $v_R([n];r)$ would be smaller.[2,58,61,62] Furthermore, it can be hoped that a judicious choice of the nonlocal operator $\hat{O}_s[\{\varphi_i\}]$ would diminish the DD to a point where quantitative comparison between the GKS LUMO energy and the electron affinity would no longer be inconceivable *a priori*. And if that were to be the case, then the GKS gap would correctly reflect the fundamental gap.

From a different perspective, recall further that we are hoping to construct a framework whereby the highest occupied and lowest unoccupied energy levels are also approximately related to the picture of lowest quasi-hole and quasi-electron excitation energies, respectively (Figure 1a). The GKS approach appears to be indispensable in this sense as well, because the nonlocal character of $\hat{O}_s[\{\varphi_i\}]$ is essential if one is to really mimic efficiently Dyson's equation, in which the self-energy operator is nonlocal by construction.[14]

Unlike the KS formalism, then, the GKS one does appear to be an eminently reasonable DFT framework, in principle, for pursuing fundamental gap calculations, at least to a satisfactory degree of approximation. The next obvious question is whether or not these ideas can be applied toward the construction of a practical, approximate GKS scheme that would be able to capitalize on its formal benefits.

## FUNDAMENTAL GAPS FROM CONVENTIONAL HYBRID FUNCTIONALS?

The most commonly employed flavor of GKS calculations, although it is seldom depicted as such, is the use of so-called "hybrid functionals".[2] In this approach, first suggested by Becke,[63] the exchange potential is described by a *fraction* of the Fock nonlocal exchange operator and a complementary fraction of a local exchange potential (typically based on GGA), in the form

$$\left(-\frac{\nabla^2}{2} + v_{ext}(r) + v_H([n];r) + a\hat{V}_F + (1-a)\,v_x^{sl}([n];r) + v_c^{sl}([n];r)\right)\varphi_i(r) = \varepsilon_i\varphi_i(r) \tag{8}$$

where $\hat{V}_F$ is the standard Fock nonlocal potential operator, namely,

$$\hat{V}_F\varphi_i(r) = -\sum_j \varphi_j(r)\int dr' \frac{1}{|r-r'|}\varphi_j^*(r')\varphi_i(r') \tag{9}$$

$a$ is the fixed fraction of Fock exchange used, and $v_x^{sl}([n];r)$ and $v_c^{sl}([n];r)$ are the approximate semilocal exchange and correlation potentials used, respectively.

The fraction employed in practice, as well as the details of the semilocal exchange and correlation potentials, can be chosen either by semiempirical fitting to a reference data set[64] or from formal considerations.[65] The "hybrid" designation reflects the fact that this approach may be viewed as a heuristic mix of the Kohn–Sham picture and the Hartree–Fock picture. But such functionals are easily placed on a rigorous footing within the GKS approach, simply by choosing $S[\{\varphi_i\}]$ to be the Slater-determinant expectation value of the sum of the kinetic energy and *a fraction of the* electron-repulsion energy operator. This yields as $\hat{O}_s[\{\varphi_i\}]$ the usual kinetic energy operator, together with a fraction of the Fock operator and the same fraction of the Hartree term. From this point of view, the rest of the Hartree term, the fraction of the local exchange potential, and the correlation potential are simply our specific choice of an approximate $v_R([n];r)$.

Unfortunately, while such conventional hybrid functionals have found a variety of uses,[2] they still do not solve the fundamental gap problem. While typically much larger than fundamental gaps derived from GGA eigenvalues, fundamental gaps derived from hybrid functional eigenvalues are still typically much smaller than the fundamental gap obtained from experimental results and/or from a GW-BSE calculation. Two examples for this observation are given in Figure 3, where two prototypical organic molecules, 3,4,9,10-perylenetetracarboxylicdianhydride (PTCDA) and free-base tetraphenylporphyrin ($H_2$TPP), are considered. For these two molecules, the HOMO–LUMO gap obtained from the popular Perdew, Burke, and Ernzerhof (PBE)[66] GGA functional are ~1.5 and 1.8 eV, respectively. As expected, these values are a huge underestimate with respect to the (experimental or GW) reference values of ~4.7 and ~5.0 eV, respectively. HOMO–LUMO gaps obtained from the popular Becke-3-parameter-Lee–Yang–Parr (B3LYP)[67] conventional hybrid functional are ~2.5 and 2.75 eV, respectively. These values are substantially larger than the PBE-derived ones but still woefully inadequate with respect to the reference values.

Partly, the unsatisfactory gaps indicate that we have not been successful in absorbing enough of the DD of the exact (and unknown) "remainder" potential, $v_R([n];r)$, into the nonlocal potential—an issue we return to below. However, even if we limit ourselves to the ionization potential alone, the results are poor, as clearly seen in Figure 3. As a second example, for $H_2O$ the ionization potential predicted from the highest occupied B3LYP orbital is lower than the experimental value by more than 4 eV.[68]

This failure is a direct consequence of using only a fraction of exact exchange. Full Fock exchange cancels the spurious electrostatic interaction of an electron with itself (known as the self-interaction error[69]) that is inherent in the Hartree term. Fractional Fock exchange only partially cancels this error. As a result, the electron is partly "repelled from itself", a fact reflected in an asymptotic binding potential that is too weak and ergo an ionization potential that is too small.[69,70]

## FUNDAMENTAL GAPS FROM RANGE-SEPARATED HYBRID FUNCTIONALS

The fact that fractional Fock-exchange GKS calculations do not offer a practical remedy for the gap problem suggests that we must seek an additional degree of flexibility in the construction of the functional form. One idea, which we found to be of particular promise, is that of the range-separated hybrid (RSH) functionals, proposed by Savin and co-workers.[71−73] In this novel class of functionals, the repulsive Coulomb potential is split into a long-range (LR) and short-range (SR) term, e.g., via $r^{-1} = r^{-1}\,\mathrm{erf}(\gamma r) + r^{-1}\,\mathrm{erfc}(\gamma r)$ (a choice that is clearly not unique—see, e.g., refs 73 and 74—but convenient). The SR and LR components are taken together in the usual way for the Hartree term, yielding the usual Hartree potential, but the components are treated differently in the generation of the exchange term. Here, we will focus on a specific subset of RSH functionals, in which the SR exchange is represented by a local potential, typically derived from a local or semilocal expression, whereas the LR part is treated via an

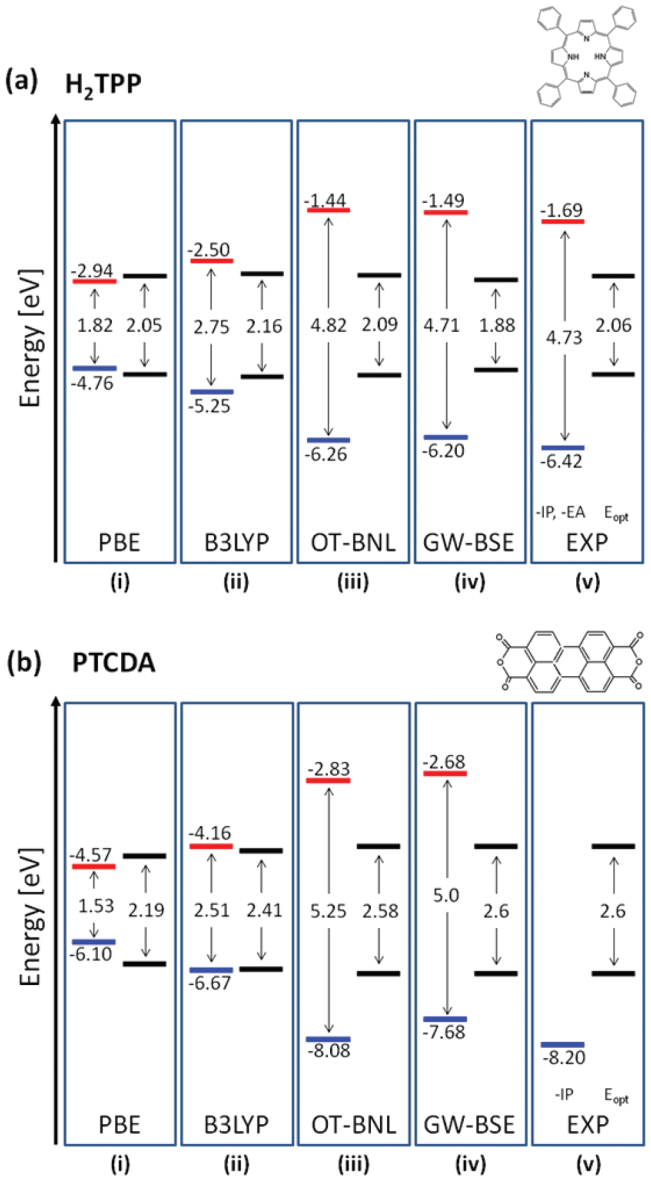


**Figure 3.** Theoretical HOMO and LUMO eigenvalues, as well as lowest optical singlet excitation energies, for (a) $H_2TPP$ and (b) PTCDA, obtained from the (i) PBE, (ii) B3LYP, and (iii) optimally tuned BNL functionals, compared to the ionization potential, electron affinity, and optical gap obtained from (iv) many-body perturbation theory using the GW-BSE method and (v) experimental results. For each method, the left-hand side shows quantities compared to the ionization potential and the electron affinity in blue and red, respectively, and the right-hand side shows quantities compared to the optical gap.[176]

"explicit" or "exact" exchange term. This leads to the following equation:

$$\left(-\frac{\nabla^2}{2} + v_{ext}(r) + v_H([n];r) + \hat{V}_F^{lr,\gamma} + v_x^{sr,\gamma}([n];r) + v_c^{sl}([n];r)\right)\varphi_i(r) = \varepsilon_i\varphi_i(r) \quad (10)$$

where $\hat{V}_F^{lr,\gamma}$ is the long-range Fock-like operator, namely

$$\hat{V}_F^{lr,\gamma}\varphi_i(r) = -\sum_j \varphi_j(r)\int dr' \frac{\mathrm{erf}(\gamma|r-r'|)}{|r-r'|}\varphi^*{}_j(r')\varphi_i(r') \quad (11)$$

and $v_x^{sr,\gamma}([n];r)$ is the SR, semilocal exchange potential. In this way, the full LR Fock exchange can be obtained, which is essential to maintaining the correct description of the asymptotic potential and therefore the ionization potential. At the same time, the use of an LDA or GGA-type SR exchange expression provides a natural way for maintaining the compatibility between exchange and correlation while still using conventional correlation expressions.

It is readily established that RSH functionals are also a special case of the GKS approach. Here, we choose $S[\{\varphi_i\}]$ to be the Slater-determinant expectation value of the sum of the kinetic energy and *the long-range* electron-repulsion energy operator, $\mathrm{erf}(\gamma r)/r$. This yields the usual kinetic energy operator, together with the LR fraction of the Fock operator and the Hartree term. Our specific choice of $v_R([n];r)$ is then the sum of the SR Hartree term, the local potential derived from the SR exchange term, and a standard correlation potential.

The parameter $\gamma$ is usually referred to as the range-separation parameter. This is because physically $1/\gamma$ can be viewed as the range below which the exchange is dominated by its SR contribution and above which the exchange is dominated by its LR contribution. The obvious question, then, is which value of $\gamma$ should we choose to use? Clearly, just as in conventional hybrid functionals, one can opt to choose $\gamma$ semiempirically; i.e., $\gamma$, possibly together with other free parameters in the local exchange and correlation terms, can be fit based on appropriate reference data. In fact, most modern RSH functionals are constructed in this way (see, e.g., refs 74−80). A significant problem, especially (but not only) in the context of determining gaps, is whether one can really think of $\gamma$ as a universal, i.e., system-independent constant. Any choice of $\gamma$ generates a legitimate approximate GKS map. However, both formal considerations[81] and practical simulations for the homogeneous electron gas problem[82] show that obtaining accurate results often requires significantly different values of $\gamma$. In fact, $\gamma$ itself can be viewed as a functional of the density,[81] of which little is known. While it is possible that other free parameters in a semiempirical RSH functional compensate for the rigid choice of $\gamma$, an issue we elaborate below, accuracy outside the training set (or even a uniform level of accuracy within it) is not guaranteed. Furthermore, the physical transparency of the RSH idea is compromised.

Can one, then, choose the range-separation parameter from physical considerations in a way that makes predictive computation of gaps possible? As stressed throughout this article, a key prerequisite is to insist explicitly that Koopmans' theorem, eq 4, be obeyed, as suggested by Livshits and Baer.[82] This means that, for each system, an optimal choice for $\gamma$ can be obtained by actively *enforcing* Koopmans' theorem,[68,82,83] i.e., by seeking a value of $\gamma$ such that

$$-\varepsilon^{\gamma}_{\mathrm{HOMO}(N)} = I^{\gamma}(N) \equiv E_{gs}(N-1;\gamma) - E_{gs}(N;\gamma) \quad (12)$$

where $\varepsilon^{\gamma}_{\mathrm{HOMO}(N)}$ is the HOMO of the $N$-electron system, per a specific choice of $\gamma$, and $I^{\gamma}(N)$ is the energy difference between the ground state energies, $E_{gs}$, of the $N$ and the $N-1$ electron systems, per the same $\gamma$. Importantly, in this way, $\gamma$ is *not* fit and the prescription is *not* semiempirical. Instead, for any choice of $\gamma$, one can compute both the left-hand and the right-hand sides of eq 12, and therefore one can seek the value of $\gamma$ for which both sides of eq 12 coincide.[86] As an example of the strength of this approach, consider the ionization potential for the set of molecules shown in Figure 4, all of which are of interest for

organic photovoltaics. Recently, the ionization potential of this set of molecules was computed using the GW approach of Blase et al.[87] Subsequently, Refaely-Abramson et al. investigated the same set with the Baer–Neuhauser–Livshits (BNL) range-separated hybrid functional,[81,82] using a range-separation parameter optimized for each molecule separately.[88] Figure 4

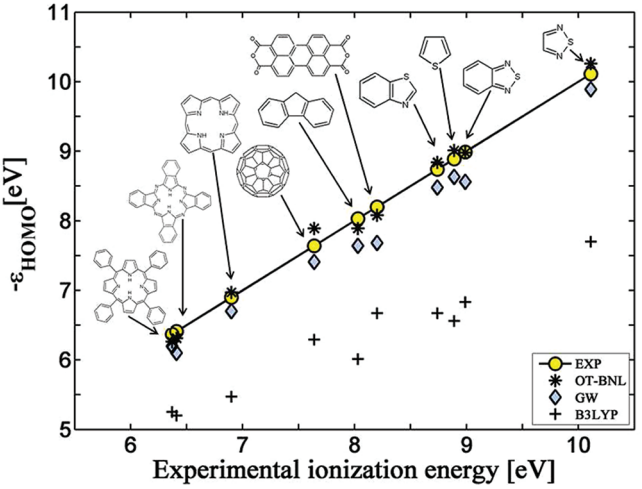


**Figure 4.** Ionization potentials for a set of photovoltaically relevant organic molecules. Circles, experimental values; stars, optimally tuned BNL values; diamonds, GW values;[87] plus signs, B3LYP values. Figure adapted with permission from the American Physical Association (ref 88).

shows that, as expected in light of the discussion in the previous section, the B3LYP highest occupied eigenvalue is an inconsistent and a serious underestimate of the experimental value, with a mean error of 1.76 eV (PBE eigenvalues do even worse and are not shown). However, the optimized BNL results compare, on average, as favorably (or even slightly more favorably) to experiment as the GW results do: The mean unsigned errors for the BNL and GW results are 0.12 and 0.3 eV, respectively.

Having demonstrated that using asymptotically correct exchange and insisting that Koopmans' theorem be obeyed allows for quantitative prediction of ionization potentials without empirical considerations, the next question to ask is whether the same can be true for the fundamental gap. For this, we also need to determine the electron affinity. As explained above, the remainder potential in eq 7 may contain a discontinuity, and therefore an analogous "Koopmans' theorem" that relates the LUMO energy to the electron affinity does not exist. This problem can be circumvented by considering, instead, $I$ of the $N + 1$ electron anion which, barring relaxation effects, is the same as $A$ of the $N$ electron system, i.e., to seek $\gamma$ such that

$$-\varepsilon^{\gamma}_{\mathrm{HOMO}(N+1)} = I^{\gamma}(N+1) \equiv E_{\mathrm{gs}}(N;\gamma) - E_{\mathrm{gs}}(N+1;\gamma) \tag{13}$$

Equations 12 and 13 provide two different conditions but only one optimization parameter, $\gamma$. The hope is that if the DD is small, the $\gamma$ implied by either conditions would be similar, so that one may simply seek to minimize the overall error by seeking to minimize a target function,[83] $J(\gamma)$, given, e.g., by

$$J^2(\gamma) = (\varepsilon^{\gamma}_{\mathrm{HOMO}(N)} + I^{\gamma}(N))^2 + (\varepsilon^{\gamma}_{\mathrm{HOMO}(N+1)} + I^{\gamma}(N+1))^2 \tag{14}$$

To examine the accuracy of this approach, Stein et al. considered the fundamental gaps for a series of atoms from the first three rows of the periodic table, computed using several functionals, and compared in Figure 5 to experimental values.[89] As expected, the PBE gaps are much smaller than the experimental ones and do not even provide a reliable qualitative guideline for the experimental trends. The B3LYP gaps are at least in some general qualitative agreement with experimental results but still underestimate them significantly. Furthermore, the difference between B3LYP and experimental results is very far from constant—as small as ~2.6 eV for Li and as large as ~9.3 eV for F. At the same time, the BNL functional, optimally tuned on the basis of eq 14, produces consistently excellent gap prediction, with a mean deviation of 0.01 eV, a mean absolute deviation of 0.1 eV, and a maximal absolute deviation of 0.3 eV (for P).

Importantly, Figure 5 also shows that different atoms require significantly different range parameters: For the alkali metal

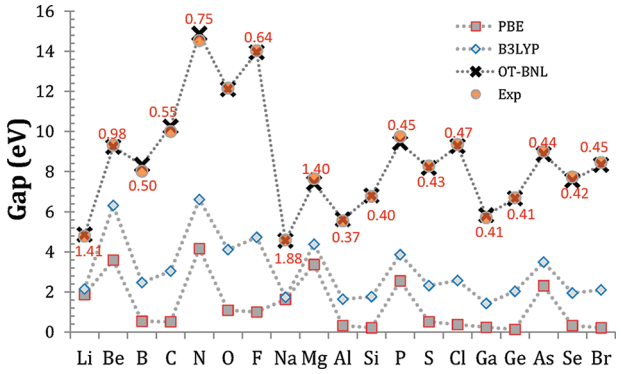


**Figure 5.** HOMO–LUMO eigenvalue gaps obtained from PBE, B3LYP, and optimally tuned BNL (with the optimal $\gamma$ value indicated near each data point), compared with experimental fundamental gaps (NIST, Reference Database No. 69 (2008)), for a variety of atoms. Figure adapted with permission from the American Physical Association (ref 89).

atoms, Li and Na, $\gamma$ is relatively high because these atoms bear more resemblance to one-electron systems where Hartree–Fock theory is exact. With the exception of Be, the general trend along a given row in the periodic table is that higher values of the gap require larger values of $\gamma$. First row atoms require values of $\gamma$ that lie between 0.5 and 0.65, whereas second and third row atoms require lower values, between 0.37 and 0.47. For a given atom, it is found that the gap is a very sensitive function of the range parameter. For example, for F and O the gap changes by as much as 8 eV when $\gamma$ changes from 0.3 to 1. This clearly shows the difficulty of yielding consistently accurate gap values with a single choice of $\gamma$, no matter what the precise details of the functional form or the training set are, and highlights the importance and nontriviality of the first-principles optimal tuning procedure.

The same optimal-tuning approach has also been found to be quantitatively useful for prediction of fundamental gaps in molecular and nanoscale systems. Stein et al. have shown that the quantum size effect, i.e., the decrease of the fundamental gap with system size, is quantitatively predicted for a series of oligoacene molecules and of hydrogenated silicon nanocrystals,[89] Refaely-Abramson et al. have shown the same for the set of molecules depicted in Figure 4.[88] These results are not shown here for brevity. However, consider again the two prototypical molecules of Figure 3—PTCDA and $H_2$TPP. Despite the above-discussed failure of the GGA and conventional hybrid approaches


dx.doi.org/10.1021/ct2009363 | J. Chem. Theory Comput. 2012, 8, 1515–1531

for determining the fundamental gap, with the optimally tuned RSH approach the fundamental gaps computed were ~5.2 and 4.8 eV, which agree with the reference values to ~0.2 eV or better.

As with atoms, molecular systems also exhibit clear chemical trends of the optimal range-separation parameter. Stein et al.,[89] Refaely-Abramson et al.,[88] and Salzner and Aydin[90] found that the optimal $\gamma$ generally decreases with system size. For example, Stein et al.[89] show that for hydrogenated Si nanocrystals, the optimal value of $\gamma$ decreases from 0.4 for the "molecular limit" of the $SiH_4$ molecule to 0.1 for a 1.3 nm nanocrystal, and in the bulk Eisenberg et al.[91] estimated an optimal $\gamma$ value on the order of 0.01. This phenomenon has been attributed to delocalization trends: As orbitals delocalize with increasing system size, semilocal approximations become more accurate, and the spatial range, $1/\gamma$, at which exact-exchange corrections are needed, becomes larger. This point of view has been confirmed and further extended by Körzdörfer et al.[92] They have studied optimal-tuning trends for a series of $\pi$-conjugated molecular systems of increasing length. For highly conjugated chains such as oligoacenes and polyenes, they found $1/\gamma$ to grow almost linearly with the number of repeat units, whereas for oligothiophenes they found that $1/\gamma$ grows linearly for the shorter oligomers but then saturates at around 10 repeat units, and for alkane chains, $1/\gamma$ saturates already after five or six repeat units. Their results thus expose a clear relation between the optimal range-separation parameter and the degree of conjugation in the system. Furthermore, again as with atoms an optimal $\gamma$ is often essential for obtaining quantitatively useful results. For example, Refaely-Abramson et al.[88] found that for the set of molecules they studied, the average unsigned error from the reference GW values for the HOMO−LUMO gap was 0.19 eV with an optimally tuned range-separation parameter but a substantially larger 0.59 eV if a universal range-separation parameter was used. A similar conclusion was drawn by Körzdörfer et al.[92] for the oligoacene series.

So far, we have examined the accuracy of the optimally tuned range-separated hybrid functional by means of comparison to experimental and many-body perturbation theory results. However, to assess its predictive power, two simple figures of merit can serve to evaluate *a priori* if the result is expected to yield a usefully accurate fundamental gap.[89] First, for the $\gamma$ that minimizes $J$ of eq 14, which we denote as $\gamma^*$, $J(\gamma^*)$ should be smaller than the desired accuracy. Second, if the DD is indeed small, than replacing $\varepsilon^{\gamma}_{\mathrm{HOMO}(N+1)}$ in eq 14 by $\varepsilon^{\gamma}_{\mathrm{LUMO}(N)}$ should yield an alternative optimization criterion:

$$J'^2(\gamma) = (\varepsilon^{\gamma}_{\mathrm{HOMO}(N)} + I^{\gamma}(N))^2 + (\varepsilon^{\gamma}_{\mathrm{LUMO}(N)} + I^{\gamma}(N+1))^2 \quad (15)$$

which should be equally useful, i.e., $\gamma'^*$ (namely, the $\gamma$ that minimizes $J'^2(\gamma)$) should be similar to $\gamma^*$ and $J'(\gamma'^*)$ should be similar to $J(\gamma^*)$.

For the above-mentioned oligoacene and the Si nanocrystal series, the tuning procedure resulted in $J(\gamma^*)$ and $J'(\gamma'^*)$ that are close to zero (~0.02 eV on average).[89] Similar results were obtained for the set of molecules shown in Figure 4. The fact that tuning based on eq 14 or eq 15 produces essentially the same results constitutes direct evidence that with the optimal range-separation parameter, the DD can indeed be driven to negligible values for these systems. Atoms are a tougher test case, because the addition or removal of a single electron changes their chemical nature appreciably, ergo it may be more difficult to find an optimal $\gamma$ that satisfies reasonably well both conditions on the right-hand side of eq 14 or eq 15. Coupled with the larger gaps atoms exhibit in general, we expect larger deviations in this case. Indeed, optimal tuning based on eq 14 or eq 15 yields an average $J'(\gamma'^*)$ or $J'(\gamma'^*)$ of 0.65 or 0.4 eV, respectively. The difference indicates a non-negligible, but still small, DD. But $J(\gamma^*)$ in this case is too harsh a criterion. The nonzero value of $J(\gamma^*)$ leads to remaining errors in $I$ and $A$ that are of the same sign, resulting in the excellent gaps of Figure 5. Thus, even in this worst-case scenario of atoms, the method still yields quantitatively useful fundamental gaps.[89]

Additional insight into the success of the optimally tuned range-separated hybrid functional approach may be gained from considering Figure 2 again. Using the same ensemble arguments discussed above in the context of KS theory, one can show that also for GKS mapping, the exact total energy versus particle number curve must be a series of linear segments as shown in Figure 2 (left). Furthermore, because Koopmans' theorem, eq 4, is equally valid for the GKS map, the interpretation of the slopes of the linear segments in Figure 2 as ionization potentials also holds. Now, Yang's group has emphasized the importance of linear segments for accurate gap prediction[79,93−95] (and see ref 86 for an additional perspective). And several groups have shown that for a well-constructed RSH functional, curves of the energy as a functional of the fractional number of electrons are much more linear than those obtained with conventional functionals.[96−98] The conditions of eq 14 or 15 then ensure that the slopes obtained would be as close as possible to the correct physical one.[92,99,100] With the contribution of the DD minimized by virtue of the nonlocal potential, this is sufficient to guarantee that the HOMO−LUMO gap obtained from the optimized functional would be directly comparable to the quasi-particle gap.

Strictly speaking, obeying the IP (Koopmans') theorem of eq 12 for an $N$-particle system is a necessary, but not sufficient, condition for obtaining a linear total energy versus particle number curve between $N-1$ and $N$ particles. It is therefore interesting to find out the extent to which tuning $\gamma$ brings us closer to the ideal linear $E(N)$ curve. We explore this in Figure 2 for $H_2O$, where we compare $E(N)$ energy curves obtained with different approaches. As mentioned above, the RSH partitioning scheme of eqs 10 and 11 is not unique. For this particular demonstration, we use the Baer−Neuhauser (BN) functional,[81] in which range separation is based on the Yukawa potential and local SR exchange and correlation are used.[102] Therefore, the BN functional reduces to the LDA one for $\gamma \to 0$ and to Hartree−Fock theory (with LDA correlation) for $\gamma \to \infty$. As shown in Figure 2 (right), in those limits of the BN functional, the results exhibit a strongly positive curvature $C \equiv \langle d^2E/dN^2 \rangle \approx 11.5$ eV and strongly negative curvature $C \approx -5$ eV, respectively, in agreement with previous studies of curvature in LDA and Hartree−Fock calculations for atoms.[103,104] Thus, there is indeed great sensitivity of the curvature to the value of $\gamma$, and remarkably, enforcing eq 12—and nothing more—already reduces the average curvature to a mere $C \approx 0.1$ eV. A similar behavior has been reported recently by Srebro and Autschbach for different molecules—$\beta$-pinene[99] and CuCl[100]—with a different underlying RSH functional, underscoring the generality of this analysis.

## OPTICAL GAPS FROM TIME-DEPENDENT KOHN–SHAM AND GENERALIZED KOHN–SHAM THEORY

DFT, in either the KS or GKS approach, is a ground state theory. Therefore, in order to consider optical excitations (or, for that matter, any other excited state property), we must look beyond DFT. The natural extension of DFT to excited states is given by time-dependent DFT (TDDFT).[33,34] The basic tenet of TDDFT is the Runge–Gross theorem,[32] which extends the Hohenberg–Kohn theorem by showing that (with reasonable restrictions on the initial states and potentials) the time-dependent density, $n(r,t)$, of a system of interacting electrons in some time-dependent external potential, $v_{ext}(r,t)$, determines this potential uniquely (up to an uninteresting, possibly time-dependent, spatially independent additive constant).

In time-dependent KS theory, one builds on the Runge–Gross theorem to show that the time-dependent density of the physical interacting-electron system can be mapped into an equivalent system of fictitious noninteracting electrons that are subject to a common *local* time-dependent external potential, in the form[32]

$$\left(-\frac{\nabla^2}{2} + v_{ext}(r,t) + v_H([n];r,t) + v_{xc}([n];r,t)\right)\varphi_i(r,t) = i\frac{\partial\varphi_i(r,t)}{\partial t} \tag{16}$$

Equation 16 is known as the time-dependent KS equation. Other than the obvious time dependence in the various quantities, the main difference between eq 16 and its time-independent counterpart, eq 2, is that the exchange-correlation potential, $v_{xc}([n];r,t)$, is now generally a functional of the entire history of the density, $n(r,t)$, as well as of the initial conditions for the many-body wave function, making it generally more complicated.

Just like the time-independent KS equation, the time-dependent KS equation is also exact in principle but approximate in practice because the exact dependence $v_{xc}([n];r,t)$ is unknown. In addition to the usual assumptions about the spatial nature of the exchange–correlation functional, one must now make a further assumption about its temporal form. In the adiabatic approximation, which is by far the one used most commonly in actual computations, one simply assumes that at any given time, the exchange–correlation potential does not depend on the history of the charge density, only on its present distribution.[105]

As discussed above, little is known about general properties of the GKS mapping. In particular, we are not aware of general theorems establishing a time-dependent GKS mapping for a completely arbitrary $S[\{\varphi_i\}]$. Fortunately, for the specific case of a mapping involving the Fock operator, including the Fock-like long-range-exchange operator discussed above, a mapping to a time-dependent GKS equation can be established by repeating the steps of the original Runge–Gross theorem in the presence of this specific nonlocal term. The time-dependent GKS equation then takes the form

$$\left(-\frac{\nabla^2}{2} + v_{ext}(r,t) + v_H([n];r,t) + v_{loc}([n];r,t) + \hat{V}_{nl}\right)\varphi_i(r,t) = i\frac{\partial\varphi_i(r,t)}{\partial t} \tag{17}$$

where the nonlocal operator, $\hat{V}_{nl}$, is $a\hat{V}_F$ of eqs 8 and 9 for a conventional hybrid functional and $\hat{V}_F^{lr,\gamma}$ of eqs 10 and 11 for an RSH functional, and $v_{loc}([n];r,t)$ represents all local-potential components of the hybrid functional used.

In most standard optical spectroscopy experiments, the perturbing electromagnetic field is weak relative to the internal fields in the probed object. Therefore, most practical applications of the time-dependent (G)KS equation are performed via linear-response theory.[106−108] In this approach, the (G)KS system is subjected to a weak perturbing time-periodic signal. Due to the self-consistent nature of the (G)KS Hamiltonian, the effective perturbation includes the response of the self-consistent potential to the perturbation. By changing the frequency of the perturbing field, this self-consistent perturbation can be used to compute the dynamic polarizability of the system. Optical excitation energies and oscillator strengths can then be computed from the poles and residues of the dynamic polarizability, respectively.

The linear response process can equivalently be viewed as the construction of a coupling matrix between all possible occupied–unoccupied ("electron-hole") pairs of (G)KS orbitals. The eigenvalues of this matrix correspond to optical excitation energies and the eigenvector components are indicative of the relative contribution of each (G)KS pair to the excitation. The optical gap is then simply the lowest eigenvalue of the coupling matrix that corresponds to a dipole-allowed transition. In the presence of a Fock-like nonlocal potential of the type discussed above, the linear-response TDDFT equation is given in the form[109]

$$\begin{pmatrix} C & D \\ -D & -C \end{pmatrix}\begin{pmatrix} X \\ Y \end{pmatrix} = \hbar\omega\begin{pmatrix} X \\ Y \end{pmatrix} \tag{18}$$

where $X$ and $Y$ are the electron–hole and hole–electron components, respectively, of the eigenvector, with

$$C_{ks\sigma,jt\sigma'} = (k_\sigma s_\sigma|r_{12}^{-1}|j_{\sigma'}t_{\sigma'}) + (k_\sigma s_\sigma|f_{\sigma\sigma'}^{\gamma}|j_{\sigma'}t_{\sigma'}) - \delta_{\sigma\sigma'}(k_\sigma j_{\sigma'}|u_\gamma(r_{12})|s_\sigma t_{\sigma'}) + (\epsilon_s - \epsilon_k)\delta_{st}\delta_{kj}\delta_{\sigma\sigma'} \tag{19}$$

and

$$D_{ks\sigma,jt\sigma'} = (k_\sigma s_\sigma|r_{12}^{-1}|t_{\sigma'}j_{\sigma'}) + (k_\sigma s_\sigma|f_{\sigma\sigma'}^{\gamma}|t_{\sigma'}j_{\sigma'}) - \delta_{\sigma\sigma'}(k_\sigma t_\sigma|u_\gamma(r_{12})|j_{\sigma'}s_\sigma) \tag{20}$$

where $\sigma$ and $\sigma'$ are spin indices, $k,j$ and $s,t$ are, respectively, indices for occupied and unoccupied (G)KS orbitals, $\varphi$, and

$$(k_\sigma s_\sigma|r_{12}^{-1}|j_{\sigma'}t_{\sigma'}) = \iint \frac{\varphi_k^\sigma(r)\,\varphi_s^\sigma(r)\,\varphi_j^{\sigma'}(r')\,\varphi_t^{\sigma'}(r')}{|r-r'|}\,d^3r\,d^3r' \tag{21}$$

$$(k_\sigma s_\sigma|f_{\sigma\sigma'}^{\gamma}|j_{\sigma'}t_{\sigma'}) = \int \varphi_k^\sigma(r)\,\varphi_s^\sigma(r)\,f_{XC}^{\gamma}(r;\sigma,\sigma')\,\varphi_j^{\sigma'}(r) \times \varphi_t^{\sigma'}(r)\,d^3r \tag{22}$$

$$(k_\sigma j_{\sigma'}|u_\gamma(r_{12})|s_\sigma t_{\sigma'}) = \iint \varphi_k^\sigma(r)\,\varphi_j^{\sigma'}(r)\,u_\gamma(|r-r'|)\,\varphi_s^\sigma(r') \varphi_t^{\sigma'}(r')\,d^3r\,d^3r' \tag{23}$$

and $f_{xc}^{\gamma}(r;\sigma,\sigma')$ is the exchange-correlation kernel (i.e., the functional derivative of the exchange-correlation potential with respect to the density), arising from the combination of the semilocal exchange and the correlation, with

$$u_\gamma(r_{12}) = \frac{\mathrm{erf}(\gamma r_{12})}{r_{12}} \tag{24}$$


dx.doi.org/10.1021/ct2009363 | J. Chem. Theory Comput. 2012, 8, 1515−1531

**Table 1. Charge Transfer Excitation Energies, in eV, for Four Donor-Tetracyanoethylene Complexes, Computed Using TDDFT with Different Functionals,[83] and GW-BSE (With[126] and Without[125] Partial Self-Consistency), Compared to Gas-Phase Experimental Data[124,a]**

| | TDDFT | | | | | GW-BSE | |
|---|---|---|---|---|---|---|---|
| donor | PBE | B3LYP | BNL ($\gamma$ = 0.5) | BNL (tuned $\gamma$) | experiment | no self-consistency | partial self-consistency |
| benzene | 1.6 | 2.1 | 4.4 | 3.8 | 3.59 | 3.2 | 3.6 |
| toluene | 1.4 | 1.8 | 4.0 | 3.4 | 3.36 | 2.8 | 3.3 |
| o-xylene | 1.0 | 1.5 | 3.7 | 3.0 | 3.15 | 2.7 | 2.9 |
| naphthalene | 0.4 | 0.9 | 3.3 | 2.7 | 2.60 | 2.4 | 2.6 |
| MAE | 2.1 | 1.7 | 0. 8 | 0.1 | | 0.4 | 0.1 |

[a]For each computation, the mean absolute error (MAE) with respect to experimental results is also given.

With straightforward modifications, these adiabatic linear-response equations are applicable to the conventional functionals discussed above as well. For semilocal functionals, one sets $u_\gamma(r_{12}) = 0$ and replaces $f^\gamma_{XC}(r;\sigma,\sigma')$ with the usual xc kernel, $f_{XC}(r;\sigma,\sigma)$. For conventional hybrid functionals, one replaces $u_\gamma(r_{12})$ with $a/r_{12}$, with $a$ as usual the hybrid mixing parameter, and replaces $f^\gamma_{XC}(r;\sigma,\sigma')$ with the appropriate local kernel of the hybrid. Linear-response time-dependent Hartree−Fock theory is also obtained as a special case, either by setting $\gamma\rightarrow\infty$ in the RSH form or by setting $a = 1$ in the conventional hybrid form and setting the xc kerenel to zero in either case.

Importantly, TDDFT, in either its KS or GKS form, is an exact theory. Indeed, the structure of the coupling matrix of eq 18 immediately shows that Coulomb and exchange-correlation interactions between filled and empty orbitals are explicitly accounted for; i.e., the requisite physics of two-body interactions is present in the linear-response formalism. Therefore, given a suitable approximation for the exchange-correlation functional, the TD−(G)KS optical gap can be meaningfully compared to experimental results even if the (G)KS gap of the underlying ground state does not correspond to the fundamental gap. Indeed, TDDFT with conventional functionals is by now well-known to produce highly satisfactory predictions of optical gaps.[34,105,110−115] However, due to the above-discussed failure of fundamental gap prediction with these functionals, the requisite two-body interaction does not conform to the physical picture of Coulomb attraction between a quasi-electron and a quasi-hole.

To understand the last statement, we return to the prototypical molecules of PTCDA and $H_2$TPP. As shown in Figure 3, for both molecules the optical gaps computed from linear-response TDDFT based on GGA, B3LYP, and optimally tuned BNL are all similar to each other and to the experimental value. However, with GGA, the KS gap is not only smaller than the fundamental gap, it is in fact substantially smaller than even the optical gap. Consequently, putting in the two-body interactions via the linear-response formalism actually *increases* the gap, contrary to the physical picture of gap reduction due to excitonic attraction. For B3LYP, the GKS gap turns out to be similar to the optical gap, and so the linear-response formalism barely changes it, again contrary to the customary physical picture. Only for the optimally tuned RSH functional, where the HOMO−LUMO gap does mimic the quasi-particle gap, is the expected gap closure obtained: the overall exciton-binding picture is the same as that obtained within many-body perturbation theory, and the quantitative values are close to those obtained from a GW+BSE calculation. Thus, the optimally tuned RSH approach retains the physical quasi-particle picture for *both* single- and two-particle excitations within one logically consistent framework, a feat not previously achieved within density functional theory.

## CHARGE TRANSFER OPTICAL EXCITATIONS FROM TIME-DEPENDENT KOHN−SHAM AND GENERALIZED KOHN−SHAM THEORY

For the intramolecular excitations of Figure 3, we have seen that the optimally tuned RSH functional approach is needed to mimic the picture of exciton binding. However, we have also seen that if one is interested in the optical gap *per se*, adiabatic linear-response TDDFT with a semilocal or conventional hybrid functional is quite sufficient. However, this is not universally true. A specific case of optical excitations, already mentioned in the Introduction, is that of the charge transfer excitation, where photon absorption induces the transfer of an electron from a donor unit to an acceptor unit. For this special but important case, use of a semilocal or a conventional hybrid functional will lead to an incorrect prediction, both quantitatively and qualitatively.

To understand why this failure occurs, we first focus on the limiting case of charge transfer between well-separated donor and acceptor units.[35,36] Consider the adiabatic linear-response TDDFT equation for the case of a singlet excitation dominated by the HOMO and LUMO orbitals, separated by a large distance $R$, such that their spatial overlap is negligible. In this limit, the matrices $C$ and $D$ of eq 18 reduce to scalars, and one can easily establish that the lowest excitation energy is given by $\varepsilon_H - \varepsilon_L - \int\int|\phi_H(r)|^2 u_\gamma(|r - r'|)|\phi_L(r')|^2\, d^3r\, d^3r'$. For the three classes of functionals considered throughout this article, this reduces to

$$\begin{aligned} &\epsilon_H - \epsilon_L && \text{semi-local functional} \\ &\epsilon_H - \epsilon_L - a/R && \text{conventional hybrid functional} \\ &\epsilon_H - \epsilon_L - 1/R && \text{RSH functional, } R \gg 1/\gamma \end{aligned} \qquad (25)$$

Now, compare these expressions to the Mulliken limit for charge transfer excitations, given in eq 1 above, $I_D - A_A - 1/R$. Identity between eq 25 and eq 1 is obtained if and only if $\varepsilon_H - \varepsilon_L$ can be equated to $I_D - A_A$ and the third term in eq 25 can be equated with $1/R$. As discussed in detail above, the eigenvalue gap is significantly smaller than the fundamental gap with either semilocal or conventional hybrid functionals. Moreover, the $1/R$ dependence is missed entirely in semilocal functionals, and only a fraction of it is accounted for in conventional hybrid functionals.[123] Both problems are cured by optimally tuned RSH functionals: they are designed to produce the correct fundamental gap, and for $1/R \ll \gamma$ the correct $1/R$ dependence is obtained inherently.


dx.doi.org/10.1021/ct2009363 | J. Chem. Theory Comput. 2012, 8, 1515−1531

With the logic of using the optimally tuned RSH functional approach established via the Mulliken limit, one must examine how well the approach works for realistic donor−acceptor distances. The success of the approach for such cases is demonstrated in Table 1. The table shows the lowest charge transfer excitation energy obtained from TDDFT with various functionals for complexes formed by an aromatic donor (benzene, toluene, *o*-xylene, and naphthalene) and the tetracyanoethylene (TCNE) acceptor,[83] compared to gas-phase experimental values[124] and to the results of two different GW-BSE calculations.[125,126] As expected from the above discussion, TDDFT with PBE clearly results in a very severe underestimate of experimental results, with a mean absolute error (MAE) of ∼2.1 eV. The results are somewhat better with B3LYP but still very far from satisfactory, with a MAE of ∼1.7 eV. In agreement with the general trends discussed above, use of BNL with its "off the shelf" default $\gamma$ value of 0.5 provides for significant further improvement, but the MAE of ∼0.8 eV is still not satisfactory. With the optimally tuned BNL functional, however, theory is consistently within ∼0.1−0.2 eV of experimental results, and the MAE is a satisfying ∼0.1 eV. Interestingly, the results obtained from the optimally tuned RSH approach are better than those obtained from "single-shot" perturbative GW corrections, followed by a BSE calculation, based on a PBE starting point. The two methods agree very well, however, if a partially self-consistent update of the quasi-particle energies when building both *G* and *W* is performed.[126]

Optimally tuned RSH-based TDDFT and GW-BSE calculations also agreed well for charge transfer energy of (substituted-anthracene)/TCNE complexes.[83,126] There, the results could only be compared to solution experiments. However, whenever a significant disagreement between theory and experiment was encountered due to solvent effects (notably for methyl and dimethyl anthracene), RSH-based TDDFT and GW-BSE results still agreed closely with each other, indicating the robustness of the optimal-tuning approach. Optimally tuned RSH-based TDDFT calculations have resulted in satisfying agreement between theory and experiment also for other donor−acceptor complexes, e.g., pentacene/$C_{60}$[127,128] and (functionalized subphthalocyanine)/$C_{60}$.[129]

Importantly, practically relevant charge separation scenarios, e.g., for photovoltaic applications, often rely on partial charge transfer from a donating moiety to an accepting moiety, rather than on complete charge transfer in a weakly bound donor−acceptor pair, owing to the larger oscillator strength of the optical absorption. Even in this case, which is further removed from the Mulliken limit, comparison of optimally tuned RSH TDDFT calculations with appropriate benchmark theoretical or experimental data reveals a significantly improved accuracy of optical gap prediction (with respect to use of conventional functionals). Successfully studied examples include, e.g., coumarin-based dyes,[130] oligothiophene-substituted naphthalene diimide,[131] and functionalized octahedral silsesquioxanes.[132]

RSH functionals in general,[133−136] and optimally tuned ones in particular,[109] were also recently found to provide quantitative accuracy in the prediction of low-lying singlet excitation energies of oligoacenes and other polyaromatic hydrocarbon systems. For this problem, semilocal and conventional hybrid functionals are indeed known to fail,[137,138] but the success of the RSH approach is surprising because the relevant transitions are clearly *not* of a charge transfer nature. Kuritz et al.[109] dubbed such excitations as "charge-transfer-like" and showed that the seemingly unrelated issue of the failure in predicting their energies is in fact strongly related to the above-discussed charge transfer problem. It is again a consequence of the presence of weakly spatially overlapping orbitals and the absence or presence of adequate nonlocal exchange. However, here the weakly spatially overlapping orbitals are not those obtained directly from the ground-state DFT calculation but rather those obtained from a unitary transformation thereof. For example, in anthracene, the optical excitation dominated by a HOMO−LUMO transition is poorly described by TDDFT with conventional functionals. The HOMO and LUMO do strongly overlap spatially, but the orbitals formed from their (normalized) sum and difference overlap spatially very weakly.[109] Thus, the bad news is that the charge-transfer-like character cannot be exposed by considering only the untransformed orbitals or the density difference induced by the excitation. The good news, however, is that the optimally tuned RSH approach inherently cures the failures associated with charge-transfer-like scenarios, even if they went undetected.

Perhaps the simplest special case of the general "charge-transfer-like" scenario, analyzed in detail by Hieringer and Görling,[139−141] is that of excitations in a spatially separated homodimer. There, the transition is dominated by four orbitals, two corresponding to a linear combination of the HOMO of each monomer and two corresponding to a linear combination of the LUMO of each monomer. Also in this case, the excitation does not involve charge-transfer that can be deduced from density differences, and yet linear-response TDDFT based on GGA fails. But a 4 × 4 unitary transformation exposes the absence of spatial overlap between the HOMO of one monomer and the LUMO of the other as the true source of this failure. Hieringer and Görling demonstrated this failure for the well-separated ethene dimer, and indeed Phillips et al.[142] recently showed that also for this system the optimally tuned RSH approach overcomes the failure, for the same reason.

Finally, we note that the optimally tuned RSH functional has also been shown recently to improve other issues associated with the description of optical excitations using TDDFT, notably the description of triplet excitations[143] (without the Tamm−Dancoff approximation[144]) and the calculation of optical rotation.[99] A detailed discussion of these interesting results is outside the scope of this article.

## THE IMPORTANCE OF OPTIMALLY TUNING A RANGE-SEPARATED HYBRID FUNCTIONAL

In the preceding sections, we showed that an optimally tuned RSH functional allows for the prediction of quantitatively accurate fundamental and optical gaps for a variety of systems. Furthermore, we explained the physical rationale that allows this achievement without recourse to empirically adjusted parameters. However, one may still wonder whether by sacrificing the absence of empiricism, one may gain equally accurate fundamental and optical gaps even without range-separation, or optimal tuning, or both. To answer this question, in this section we consider three classes of alternative exchange-correlation functionals that could potentially be viewed as viable candidates for gap calculations within a GKS scheme.

The first class consists of short-range ("screened") hybrid functionals[145,146] and is best exemplified by the Heyd, Scuseria, and Ernzerhof (HSE) functional.[147,148] In this approach, the

Coulomb repulsion operator is partitioned into SR and LR components using the error function, as explained above. However, unlike in the RSH scheme of eqs 10 and 11, a conventional-hybrid *fraction* of Fock exchange is used *in the SR only*, with *no LR Fock exchange*. Specifically for HSE, the Fock fraction is a nonempirical $a = 0.25$, adapted from the PBE-based conventional hybrid (PBE0[65,149,150]), and $\gamma$ is determined empirically to be 0.11, based on its performance for extensive training sets. It is interesting to examine HSE-based gaps for finite systems, because for many bulk solids the HSE HOMO−LUMO gap has been found to be in very good agreement with experimental gap values.[151−153]

The second class we examine consists of semiempirical conventional hybrid functionals, whose functional forms for the various exchange and correlation components contain a (possibly large) number of empirical parameters. These parameters are fixed by fitting to a large and diverse training set, with the aim of providing a balanced treatment of main group thermochemistry and kinetics, transition metal chemistry, long-range charge transfer, and noncovalent interactions. As an example for this class, we consider here the M06 set of functionals,[154,155] a family of meta-GGA-based functionals (i.e., functionals whose "semi-local" component includes kinetic energy spin densities, in addition to the spin-densities and their gradients[2]), with varying fractions of exact exchange, and several dozen additional empirical parameters in the functional form. Here, we consider two members of the M06 family: (1) M06, recommended as having the best "across-the-board" accuracy,[154] which is comparable to B3LYP or PBE0 in terms of its fraction of exact exchange ($a = 0.27$), and (2) M06-HF,[156] which has full Fock exchange ($a = 1$) and therefore exhibits the correct asymptotic potential, but with some sacrifice of ground state accuracy.[154] It is interesting to examine M06 to see if the large degree of empiricism assists gap predictions, and it is interesting to examine M06-HF in order to test the extent to which it improves gap predictions owing to its correct asymptotic potential.

The third class of functionals we consider consists of long-range RSH functionals, but with $\gamma$ determined semiempirically once and for all, rather than tuned per system. Of those, we consider here two representative functionals—LC-$\omega$PBE, a PBE-based long-range RSH,[76,157] and $\omega$B97X, a B97-based long-range RSH that also includes a fraction of short-range Fock exchange.[75] The former is "in the spirit of HSE" in the sense that its $\gamma = 0.4$ is the only empirically fit parameter. The latter is "in the spirit of the M06 family" in the sense that it contains 16 additional fitting parameters, other than its $\gamma = 0.3$. Both functionals have been found to do well for a broad range of molecular properties. It is interesting to examine these functionals so as to test to what degree their universal range-separation parameter, possibly augmented with additional flexibility in the functional form, can provide sufficient accuracy for various systems.

To facilitate a comparison between the different approaches, we revisit the systems studied in Figures 3−5, namely, the fundamental gaps of atoms, the ionization potentials for a set of photovoltaically relevant organic molecules, and the fundamental and optical gaps of our two prototypical molecules, PTCDA and $H_2$TPP—all with the same basis sets used in the original articles.[88,89] The results are presented in Figure 6a−c.

Many observations are drawn from Figure 6. First, it is clear that HSE and M06 are essentially equivalent to B3LYP: using their eigenvalues to predict ionization potentials and fundamental gaps results in qualitatively identical and quantitatively similar underestimates, while the optical gap obtained from TDDFT is very close. In other words, the fraction of Fock exchange is the primary factor in gap determination, with elimination of long-range exchange or semiempirical optimization of other exchange and correlation components playing a secondary role. For HSE in particular, it has been repeatedly observed (see, e.g., refs 153, 158−162) that gaps derived from the HSE HOMO−LUMO gap are often close to the optical gap, rather than the fundamental one. Figure 6c shows that this is true also for PTCDA and $H_2$TPP, but still a time-dependent HSE is required for quantitative accuracy. In any case, neither HSE nor M06 provide the above-discussed desired physical picture of gap reduction due to excitonic attraction.

In principle, one can consider whether this limitation can be overcome by tuning the fraction of exact exchange in a conventional hybrid functional (namely, the parameter $a$ of eq 8), so as to minimize the curvature of the total energy versus particle number curve. This procedure has in fact been employed recently by Sai et al.[163] For small oligoacenes, they found that for PBE0 (where usually[65] $a = 0.25$) this procedure leads to $a = 0.75$, which results in improved gap predictions and an improved description of hole localization in the molecular solid. Similar behavior has been found by Imamura et al. for other small molecules and other underlying functionals.[164] We note, however, that such a large fraction of exact exchange is above-and-beyond that known to result in quantitative predictions of thermochemical[149,150,154] or electronic structure[165,166] properties. Thus, obtaining quantitatively accurate ionization potentials and quasi-particle gaps from conventional hybrid functionals, without disrupting the delicate balance between exchange and correlation in ways that could be otherwise detrimental, appears to be very difficult indeed.

Consider now the M06-HF functional, which is still a conventional hybrid functional "in spirit" but is unusual in having the full Fock exchange. For atoms, we have encountered serious convergence issues with M06-HF. Therefore, M06-HF data do not appear in Figure 6a. Clearly, M06-HF does offer some quantitative improvement over M06 for the ionization potentials in Figure 6b (reducing the mean error from ∼1.6 eV to ∼0.9 eV). Importantly, whereas M06 consistently underestimates ionization potentials, M06-HF consistently overestimates them. For the fundamental gaps in Figure 6c, the quantitative improvement is much more significant. Furthermore, considering the optical gaps as well, the physical picture of gap reduction due to excitonic attraction is now obtained, emphasizing yet again the importance of utilizing functionals that yield the correct asymptotic potential. Unfortunately, M06-HF again results in an overestimate of the experimental and/or many-body perturbation theory results, by an unsatisfying ∼1 eV.

Overestimation of ionization potential and fundamental gaps is qualitatively typical of Hartree−Fock calculations. We interpret this behavior of M06-HF as indicative of the difficulty of obtaining sufficiently accurate correlation expressions that are compatible with full exact exchange, even with extensive empiricism. Such compatibility is quite generally a very difficult task, because it inherently requires a highly nonlocal dependence of the correlation on the density,[2] and its absence is the Achilles heel of M06-HF. Consequently, while gap prediction from M06-HF eigenvalues offers both qualitative and quantitative advantages over other hybrid functionals, this comes at the cost of M06-HF being inferior to other hybrid functionals for other ground state properties, and despite this

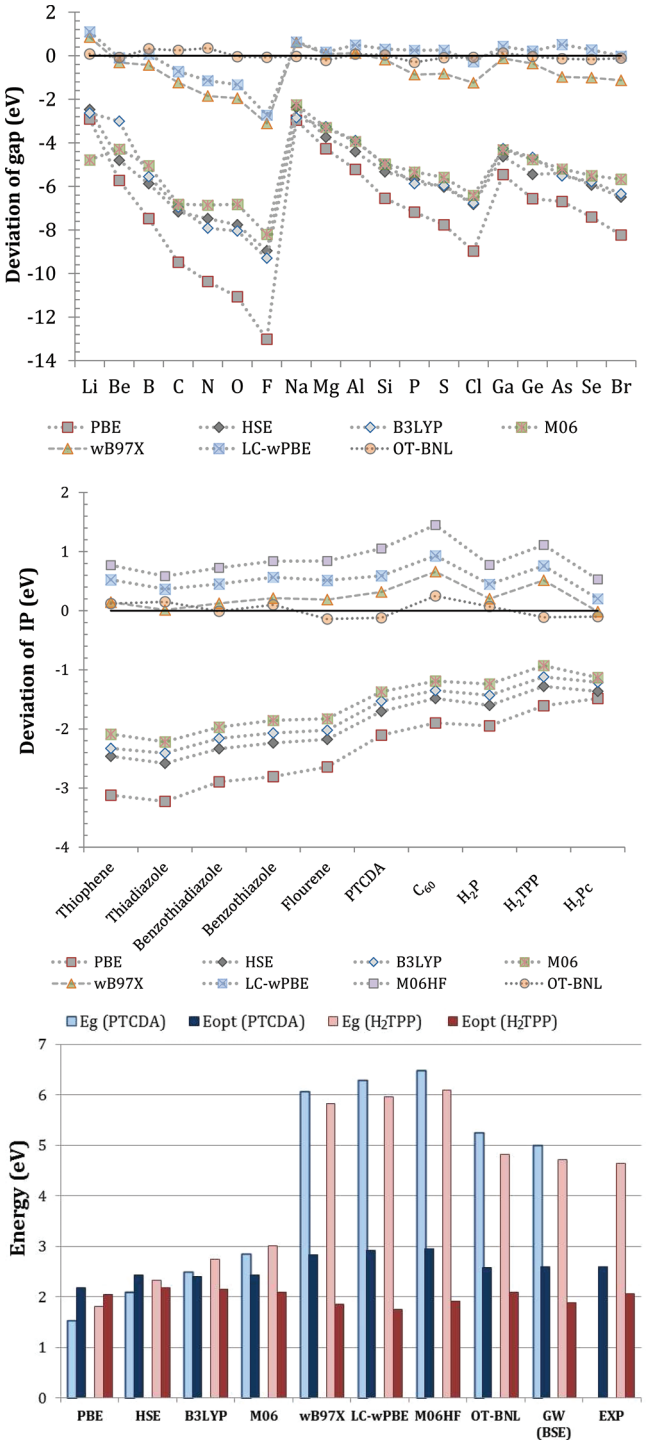


**Figure 6.** Comparative study of error trends obtained from the different functionals discussed in the text. (a) Difference between HOMO−LUMO eigenvalue gaps and experimental fundamental gaps for a variety of atoms. (b) Difference between HOMO eigenvalue and experimental ionization potential for a set of photovoltaically relevant organic molecules. (c) Fundamental and optical gaps for PTCDA and $H_2$TPP, compared to many-body perturbation theory and experimental values.

sacrifice its gap results are still quantitatively unsatisfying. This naturally points to RSH functionals which, as discussed above, provide a natural way for maintaining the compatibility between exchange and correlation.

The remaining question, then, is whether tuning of RSH functionals is really essential for gap prediction, or whether it can be circumvented by fitting of the range-separation and other parameters. Consider, then, the performance of LC-$\omega$PBE and $\omega$B97X. For the atomic gaps of Figure 6a, both functionals provide a dramatic improvement in accuracy over conventional hybrid functionals, in agreement with previous studies on the performance of nontuned RSH functionals for atomic gaps.[96,98] However, quantitatively both still exhibit a significant error—as large as ∼3 eV for F. More interestingly, they exhibit a qualitative problem similar to that of conventional hybrid functionals, namely, a clear error trend across rows of the periodic table, especially the first one. This trend does not exist in the optimally tuned BNL results, a fact which we attribute directly to the strong variations in the optimal range-separation parameter across the first row of the periodic table (cf. Figure 5). Complementarily, while optimally tuned BNL results are superior throughout, LC-$\omega$PBE results are closest to them for the heavier elements, where its range-separation parameter ($\gamma$ = 0.4) is generally close to the optimized value.

For the molecular ionization potentials of Figure 6b, both of the semiempirical RSH functionals again provide a dramatic improvement in accuracy over conventional hybrid functionals, as well as a significant quantitative improvement over M06-HF. Still, their results clearly fall short of those obtained by optimal tuning. Unlike the atomic case, here it is $\omega$B97X, rather than LC-$\omega$PBE, which is closer to experimental results. We attribute this to its smaller range-separation parameter ($\gamma$ = 0.3), which is more appropriate for these systems, as well as to its additional empirical parameters. Most importantly, Figure 6c shows that, as expected, both functionals provide the physical picture of gap reduction due to excitonic attraction, but neither is quantitatively useful—for PTCDA, for example, the predicted fundamental gap is off the GW value by ∼1 eV and is only marginally better than that obtained from M06-HF. This can be further understood by considering the series of hydrogenated Si nanocrystals mentioned above.[89] For the $SiH_4$ molecule, we find that $\omega$B97X predicts a gap that is within a satisfying ∼0.2 eV from the reference GW value. However, for the larger $Si_{35}H_{36}$ passivated nanocrystal, the same functional predicts a gap that overestimates the GW reference data by an entirely unsatisfying ∼2.1 eV—a direct consequence of the failure of a fixed range-separation parameter to follow the delocalization trends discussed in previous sections. Thus, we find that for all functionals tested the additional degrees of empiricism are not capable of reaching the accuracy afforded by optimal tuning of the range-separation parameter.

As explained above on the basis of the Mulliken limit, correct prediction of the fundamental gap is essential to the correct prediction of charge transfer optical excitations. Thus, it comes as no surprise that the above-discussed trends recur upon revisiting the charge-transfer excitations of Table 1. We do not provide the full results for brevity, but as before, HSE and M06 are essentially equivalent to B3LYP, whereas M06-HF provides an overestimate of excitation energies. Here, it is important to point out that in recent years a significant body of literature, too vast to review here in detail (but see, e.g., refs 75, 133, 167−172 for some examples), has shown that empirically constructed RSH functionals greatly improve the prediction of (full or partial) charge transfer excitation energies, often reaching quantitative agreement with experimental results. For the test systems of Table 1, we too find that the semiempirical RSH functionals provide for further improvement, but that they


dx.doi.org/10.1021/ct2009363 | J. Chem. Theory Comput. 2012, 8, 1515−1531

become quantitatively accurate only if their range-separation parameter happens to be appropriate. Similar findings as to the importance of tuning for the quantitative accuracy of RSH functionals have been recently given by Minami et al. for the pentacene/$C_{60}$ complex.[128]

Specifically, we believe that several important advantages are associated with using optimally tuned, rather than empirical, RSH functionals, for charge-transfer excitations. First, optimal tuning allows for computation of accurate excitation energies without the introduction of any empirical parameters or fitting procedures—an important issue for obtaining truly predictive power even for systems sufficiently different from those in the training set. Second, it naturally overcomes the fact that the value of $\gamma$ that is optimal for, e.g., thermochemistry may not necessarily be the one optimal for excited state properties[61,78,173] (and cf. Table 1). Last but not least, with optimal tuning, the underlying physics—fulfillment of the Mulliken limit via explicit enforcement of eq 25—is transparent and not obscured by additional constructs in the exchange and/or correlation functionals.

To summarize, while one can never rule out future ingenuity, presently non-RSH functionals, as well as RSH functionals that are not optimally tuned, do not offer satisfactory quantitative prediction of fundamental and optical gaps for a sufficiently wide variety of systems, even if one is willing to embrace empiricism.

## CONCLUDING REMARKS

The most important message of this article is that in finite systems, contrary to conventional wisdom, both single- and two-quasi-particle excitation thresholds can be reliably predicted from the HOMO−LUMO eigenvalue difference of a DFT calculation and the lowest eigenvalue of a TDDFT calculation, respectively, using the same exchange-correlation functional.

Throughout this article, we have attempted to show that this newly discovered capability, which conventional semilocal and hybrid functionals do not possess, is made possible by nesting three essential concepts, each of which removes a different obstacle. The first essential concept is the generalized Kohn−Sham scheme. It provides the hope for minimizing the role of the derivative discontinuity, which precluded the identification of the HOMO−LUMO gap with the fundamental gap in the original Kohn−Sham approach. Within the generalized Kohn−Sham scheme, the second essential concept is that of the range-separated hybrid functional. It allows us to bridge two requirements—the need for exact exchange so as to obtain the correct asymptotic potential and the notoriously difficult need to devise computationally convenient correlation expressions that would be compatible with exact exchange. In the range-separated hybrid scheme, the semilocal correlation provides a quantitative approximation of the dynamic correlation, whereas the short-range semilocal exchange also mimics the static correlation, such that a useful balance of all exchange and correlation components can be obtained in a natural manner.

From an exchange-correlation energy point of view, the range-separated hybrid functional belongs in the fourth rung of Perdew's famous "Jacob's ladder" classification of density functionals[174]—it is an explicitly orbital-dependent functional, which uses the density and its gradient along with filled orbitals, so as to create an approximation for what can effectively be viewed as exact exchange with approximate compatible correlation. As such, it may still be used in two different ways:[2] (1) within the Kohn−Sham scheme, where the corresponding local (multiplicative) exchange-correlation potential is derived by taking the functional derivative with respect to the *density* using the optimized effective potential equation, and (2) within the generalized Kohn−Sham scheme, where the nonlocal component of the exchange-correlation potential is derived by taking the functional derivative with respect to the *orbitals*. We emphasize again that only the generalized Kohn−Sham scheme, however, is suitable for describing single-quasi-particle excitations based on frontier eigenvalues, underscoring the need to combine the first two essential concepts.

Within the range-separated hybrid functional approach, the third essential concept is the use of system-specific optimal tuning to determine the range separation parameter. It is needed because it allows us to overcome the difficulty of the absence of a universal, system-independent value for a range-separation parameter. By providing us with a natural, physically motivated procedure for finding a system-dependent range-separation parameter, the correct balance between exchange and correlation is attained for any system of interest. However, the optimal tuning idea is more than just a mathematical device. Fundamentally, we view it as a significant departure from the usual paradigm for functional construction and application. Typically within DFT, we seek an increasingly general functional form that can come as close as possible to the ideal of a universal functional. The price to pay for that, however, is an increasingly complex functional and an increasingly larger computational cost (a fact made clear from, e.g., consideration of the different rungs in the above-mentioned "Jacob's ladder" of functionals). Here, we choose to sacrifice the notion that we always seek an all-purpose functional expression—the theoretical equivalent of a "Swiss army knife"—so as to gain greatly in simplicity and applicability without a loss of accuracy. Specifically, we gain by retaining a reasonably simple, low-cost functional form (i.e., that of eq 10). In return, we pay the relatively modest price of the system-specific tuning step, through which we retrieve the flexibility that was lost in the choice of the functional form. Importantly, we sacrifice neither the predictive power nor the first principles nature of the approach. This is because we do not *fit* the parameter against a set of empirical data but rather *tune* it so as to uphold a physical requirement.

At this point, we need to emphasize that the above approach is not a panacea. Many challenges remain, some of which we briefly sketch here. First of all, throughout this text we have focused on excitation thresholds only and have not addressed higher energy excitations. Second, a major limitation is that the approach is not size consistent. This means that if we take a system comprised of two well-separated and different subunits, the total energy of the system is not guaranteed to be the sum of the total energy for each separately calculated subunit, due to a possibly different optimal choice of the range-separation parameter. This failure severely limits binding energy calculations. More generally, it is expected to limit the accuracy of the approach for significantly heterogeneous systems where different moieties may require different effective range-separation parameters. Third, the approach as given here is applicable to finite-sized systems. For periodic systems, such as solids, or partially periodic systems such as surfaces, nanowires, or nanotubes, adding or removing an electron explicitly is not possible due to periodic boundary conditions. Last but not least, in some cases, quantitative differences with respect to experimental results may remain (see, e.g., refs 90 and 99), and in other cases (e.g., systems with a strong multireference character), the performance of the approach has not been

sufficiently investigated yet. We attribute such difficulties to the delicate balance between the remaining exchange and correlation components.

Despite these remaining limitations and others, we do believe that the approach presented in this article provides a useful intellectual and practical framework for further research, development, and application. Consider that in their 2002 overview on density-functional versus many-body Green's function approaches to electronic excitations, Onida et al. pointed out that "progress in the theoretical description of spectroscopy is in fact very often linked to progress in finding better effective one- or two particle Hamiltonians".[1] We find that this is precisely what the work presented here accomplishes and, in doing so, provides a major step forward in bridging the typical chasm between the DFT and the quasi-particle point of view. Specifically, we have provided a procedure for determining an effective one-particle Hamiltonian within DFT, which is "better" in the sense of it being able to mimic single-quasiparticle many-body perturbation theory more effectively. Furthermore, within TDDFT, the linear-response kernel based on the same approach allows us to mimic the two-particle interaction in general and the exciton binding energy in particular. This opens the door for reliable theoretical spectroscopy for a great variety of systems that are computationally out of reach for many-body perturbation theory techniques.

## AUTHOR INFORMATION


### Corresponding Author

*E-mail: leeor.kronik@weizmann.ac.il; roi.baer@huji.ac.il.


### Notes

The authors declare no competing financial interest.

## ACKNOWLEDGMENTS

Work at the Weizmann Institute was supported by the European Research Council, the Israel Science Foundation, the Lise Meitner Minerva Center for Computational Chemistry, and the historic generosity of the Perlman family. Work at the Hebrew University was supported by the Israel Science Foundation and the U.S.−Israel Binational Science Foundation.

## REFERENCES


(1) Onida, G.; Reining, L.; Rubio, A. *Rev. Mod. Phys.* **2002**, *74*, 601−659.
(2) Kümmel, S.; Kronik, L. *Rev. Mod. Phys.* **2008**, *80*, 3−60.
(3) Landau, L. D. *Sov. Phys. JETP* **1957**, *3*, 920.
(4) Mulliken, R. S. *J. Am. Chem. Soc.* **1952**, *74*, 811−824.
(5) Dreuw, A.; Head-Gordon, M. *Chem. Rev.* **2005**, *105*, 4009−4037.
(6) Sekino, H.; Bartlett, R. J. *Int. J. Quantum Chem.* **1984**, *26*, 255−265.
(7) Christiansen, O.; Koch, H.; Jørgensen, P. *Chem. Phys. Lett.* **1995**, *243*, 409−418.
(8) Foresman, J. B.; Head-Gordon, M.; Pople, J. A.; Frisch, M. J. *J. Phys. Chem.* **1992**, *96*, 135−149.
(9) Krylov, A. I. *Annu. Rev. Phys. Chem.* **2008**, *59*, 433−462.
(10) Rienstra-Kiracofe, J. C.; Tschumper, G. S.; Schaefer, H. F.; Nandi, S.; Ellison, G. B. *Chem. Rev.* **2002**, *102*, 231−282.
(11) Grossman, J. C.; Rohlfing, M.; Mitas, L.; Louie, S. G.; Cohen, M. L. *Phys. Rev. Lett.* **2001**, *86*, 472−475.
(12) Williamson, A. J.; Grossman, J. C.; Hood, R. Q.; Puzder, A.; Galli, G. *Phys. Rev. Lett.* **2002**, *89*, 196803.
(13) Kolorenc, J.; Mitas, L. *Rep. Prog. Phys.* **2011**, *74*, 026502.
(14) Strinati, G. *Riv. Nuovo Cimento* **1988**, *11*, 1−86.
(15) Dyson, F. J. *Phys. Rev.* **1949**, *75*, 1736.
(16) Hedin, L. *Phys. Rev.* **1965**, *139*, A796−A823.
(17) Hybertsen, M. S.; Louie, S. G. *Phys. Rev. B* **1986**, *34*, 5390−5413.
(18) Aryasetiawan, F.; Gunnarsson, O. *Rep. Prog. Phys.* **1998**, *61*, 237−312.
(19) Salpeter, E. E.; Bethe, H. A. *Phys. Rev.* **1951**, *84*, 1232−1242.
(20) Rohlfing, M.; Louie, S. G. *Phys. Rev. B* **2000**, *62*, 4927−4944.
(21) Samsonidze, G.; Jain, M.; Deslippe, J.; Cohen, M. L.; Louie, S. G. *Phys. Rev. Lett.* **2011**, *107*, 186404.
(22) Gross, E. K. U.; Dreizler, R. M. *Density Functional Theory*; Plenum Press: New York, 1995; pp xiv, 676.
(23) Parr, R. G.; Yang, W. *Density Functional Theory of Atoms and Molecules*; Oxford University Press: Oxford, U. K., 1989.
(24) Sholl, D. S.; Steckel, J. A. *Density Functional Theory: A Practical Introduction*; Wiley: Hoboken, NJ, 2009.
(25) Koch, W.; Holthausen, M. C. *A Chemist's Guide to Density Functional Theory*; Wiley: Heidelberg, Germany, 2001.
(26) Martin, R. M. *Electronic Structure: Basic Theory and Practical Methods*; Cambridge University Press: Cambridge, U.K., 2004.
(27) Sham, L. J.; Schlüter, M. *Phys. Rev. Lett.* **1983**, *51*, 1888−1891.
(28) Perdew, J. P.; Levy, M. *Phys. Rev. Lett.* **1983**, *51*, 1884−1887.
(29) Toher, C.; Filippetti, A.; Sanvito, S.; Burke, K. *Phys. Rev. Lett.* **2005**, *95*, 146402.
(30) Cehovin, A.; Mera, H.; Jensen, J. H.; Stokbro, K.; Pedersen, T. B. *Phys. Rev. B* **2008**, *77*, 195432.
(31) Quek, S. Y.; Choi, H. J.; Louie, S. G.; Neaton, J. B. *Nano Lett.* **2009**, *9*, 3949−3953.
(32) Runge, E.; Gross, E. K. U. *Phys. Rev. Lett.* **1984**, *52*, 997−1000.
(33) Marques, M.; Maitra, N. T.; Nogueira, F.; Gross, E. K. U.; Rubio, A. *Fundamentals of Time-Dependent Density Functional Theory*; Springer: Berlin, 2012.
(34) Ullrich, C. A. *Time-Dependent Density-Functional Theory: Concepts and Applications*; Oxford University Press: Oxford, U. K., 2012.
(35) Dreuw, A.; Weisman, J. L.; Head-Gordon, M. *J. Chem. Phys.* **2003**, *119*, 2943−2946.
(36) Tozer, D. J. *J. Chem. Phys.* **2003**, *119*, 12697−12699.
(37) Hohenberg, P.; Kohn, W. *Phys. Rev.* **1964**, *136*, B864.
(38) Kohn, W.; Sham, L. J. *Phys. Rev.* **1965**, *140*, A1133.
(39) Chong, D. P.; Gritsenko, O. V.; Baerends, E. J. *J. Chem. Phys.* **2002**, *116*, 1760−1772.
(40) Gritsenko, O. V.; Baerends, E. J. *J. Chem. Phys.* **2002**, *117*, 9154−9159.
(41) Perdew, J. P.; Parr, R. G.; Levy, M.; Balduz, J. L. *Phys. Rev. Lett.* **1982**, *49*, 1691−1694.
(42) Almbladh, C.-O.; von-Barth, U. *Phys. Rev. B* **1985**, *31*, 3231−3244.
(43) Perdew, J. P.; Levy, M. *Phys. Rev. B* **1997**, *56*, 16021−16028.
(44) Levy, M.; Perdew, J. P.; Sahni, V. *Phys. Rev. A* **1984**, *30*, 2745−2748.
(45) Koopmans, T. C. *Physica* **1934**, *1*, 104.
(46) Sagvolden, E.; Perdew, J. P. *Phys. Rev. A* **2008**, *77*, 012517.
(47) Gunnarsson, O.; Schönhammer, K. *Phys. Rev. Lett.* **1986**, *56*, 1968−1971.
(48) Godby, R. W.; Schluter, M.; Sham, L. J. *Phys. Rev. Lett.* **1986**, *56*, 2415−2418.
(49) Chan, G. K.-L. *J. Chem. Phys.* **1999**, *110*, 4710−4723.
(50) Allen, M. J.; Tozer, D. J. *Mol. Phys.* **2002**, *100*, 433−439.
(51) Janak, J. *Phys. Rev. B* **1978**, *18*, 7165−7168.
(52) Teale, A. M.; De Proft, F.; Tozer, D. J. *J. Chem. Phys.* **2008**, *129*, 044110−12.
(53) Borgoo, A.; Teale, A. M.; Tozer, D. J. *J. Chem. Phys.* **2012**, *136*, 034101−6.
(54) Tozer, D. J. *Phys. Rev. A* **1998**, *58*, 3524−3527.
(55) Chan, M. K. Y.; Ceder, G. *Phys. Rev. Lett.* **2010**, *105*, 196403.
(56) Mera, H.; Stokbro, K. *Phys. Rev. B* **2009**, *79*, 125109.
(57) Andrade, X.; Aspuru-Guzik, A. *Phys. Rev. Lett.* **2011**, *107*, 183002.
(58) Seidl, A.; Görling, A.; Vogl, P.; Majewski, J. A.; Levy, M. *Phys. Rev. B* **1996**, *53*, 3764−3774.

(59) Görling, A.; Levy, M. *J. Chem. Phys.* **1997**, *106*, 2675−2680.
(60) Handy, N. C.; Marron, M. T.; Silverstone, H. J. *Phys. Rev.* **1969**, *180*, 45−48.
(61) Baer, R.; Livshits, E.; Salzner, U. *Annu. Rev. Phys. Chem.* **2010**, *61*, 85−109.
(62) Grüning, M.; Marini, A.; Rubio, A. *Phys. Rev. B* **2006**, *74*, 161103.
(63) Becke, A. D. *J. Chem. Phys.* **1993**, *98*, 1372−1377.
(64) Becke, A. D. *J. Chem. Phys.* **1993**, *98*, 5648−5652.
(65) Perdew, J. P.; Ernzerhof, M.; Burke, K. *J. Chem. Phys.* **1996**, *105*, 9982−9985.
(66) Perdew, J. P.; Burke, K.; Ernzerhof, M. *Phys. Rev. Lett.* **1996**, *77*, 3865−3868.
(67) Stephens, P. J.; Devlin, F. J.; Chabalowski, C. F.; Frisch, M. J. *J. Phys. Chem.* **1994**, *98*, 11623−11627.
(68) Salzner, U.; Baer, R. *J. Chem. Phys.* **2009**, *131*, 231101−4.
(69) Perdew, J. P.; Zunger, A. *Phys. Rev. B* **1981**, *23*, 5048−5079.
(70) van Leeuwen, R.; Baerends, E. J. *Phys. Rev. A* **1994**, *49*, 2421−2431.
(71) Savin, A. Beyond the Kohn-Sham Determinant. In *Recent Advances in Density Functional Methods Part I*; Chong, D. P., Ed.; World Scientific: Singapore, 1995; p 129.
(72) Leininger, T.; Stoll, H.; Werner, H.-J.; Savin, A. *Chem. Phys. Lett.* **1997**, *275*, 151−160.
(73) Savin, A.; Flad, H. J. *Int. J. Quantum Chem.* **1995**, *56*, 327−332.
(74) Iikura, H.; Tsuneda, T.; Yanai, T.; Hirao, K. *J. Chem. Phys.* **2001**, *115*, 3540−3544.
(75) Chai, J. D.; Head-Gordon, M. *J. Chem. Phys.* **2008**, *128*, 084106.
(76) Vydrov, O. A.; Scuseria, G. E. *J. Chem. Phys.* **2006**, *125*, 234109.
(77) Yanai, T.; Tew, D. P.; Handy, N. C. *Chem. Phys. Lett.* **2004**, *393*, 51−57.
(78) Rohrdanz, M. A.; Martins, K. M.; Herbert, J. M. *J. Chem. Phys.* **2009**, *130*, 054112.
(79) Cohen, A. J.; Mori-Sanchez, P.; Yang, W. T. *J. Chem. Phys.* **2007**, *126*, 191109.
(80) Chai, J. D.; Head-Gordon, M. *Phys. Chem. Chem. Phys.* **2008**, *10*, 6615−6620.
(81) Baer, R.; Neuhauser, D. *Phys. Rev. Lett.* **2005**, *94*, 043002.
(82) Livshits, E.; Baer, R. *Phys. Chem. Chem. Phys.* **2007**, *9*, 2932−2941.
(83) Stein, T.; Kronik, L.; Baer, R. *J. Am. Chem. Soc.* **2009**, *131*, 2818−2820.
(84) Lany, S.; Zunger, A. *Phys. Rev. B* **2009**, *80*, 085202.
(85) Dabo, I.; Ferretti, A.; Poilvert, N.; Li, Y. L.; Marzari, N.; Cococcioni, M. *Phys. Rev. B* **2010**, *82*, 115121.
(86) A somewhat related but different strategy, based on per orbital corrections following a generalized Koopmans' approach, is discussed in refs 84 and 85.
(87) Blase, X.; Attaccalite, C.; Olevano, V. *Phys. Rev. B* **2011**, *83*, 115103.
(88) Refaely-Abramson, S.; Baer, R.; Kronik, L. *Phys. Rev. B* **2011**, *84*, 075144.
(89) Stein, T.; Eisenberg, H.; Kronik, L.; Baer, R. *Phys. Rev. Lett.* **2010**, *105*, 266802.
(90) Salzner, U.; Aydin, A. *J. Chem. Theory Comput.* **2011**, *7*, 2568−2583.
(91) Eisenberg, H. R.; Baer, R. *Phys. Chem. Chem. Phys.* **2009**, *11*, 4674−4680.
(92) Körzdörfer, T.; Sears, J. S.; Sutton, C.; Bredas, J.-L. *J. Chem. Phys.* **2011**, *135*, 204107−6.
(93) Mori-Sanchez, P.; Cohen, A. J.; Yang, W. T. *Phys. Rev. Lett.* **2008**, *100*, 146401.
(94) Zheng, X.; Cohen, A. J.; Mori-Sánchez, P.; Hu, X.; Yang, W. *Phys. Rev. Lett.* **2011**, *107*, 026403.
(95) Cohen, A. J.; Mori-Sánchez, P.; Yang, W. *Chem. Rev.* **2012**, *112*, 289−320.
(96) Cohen, A. J.; Mori-Sanchez, P.; Yang, W. T. *Phys. Rev. B* **2008**, *77*, 115123.
(97) Vydrov, O. A.; Scuseria, G. E.; Perdew, J. P. *J. Chem. Phys.* **2007**, *126*, 154109.
(98) Tsuneda, T.; Song, J. W.; Suzuki, S.; Hirao, K. *J. Chem. Phys.* **2010**, 133. Imamura, Y.; Kobayashi, R.; Nakai, H. *J. Chem. Phys.* **2011**, *134*, 124113.
(99) Srebro, M.; Autschbach, J. *J. Chem. Theory Comput.* **2011**, *8*, 245−256.
(100) Srebro, M.; Autschbach, J. *J. Phys. Chem. Lett.* **2012**, *3*, 576−581.
(101) Troullier, N.; Martins, J. L. *Phys. Rev. B* **1991**, *43*, 1993−2006.
(102) The calculations were performed using a planewave basis in conjunction with norm-conserving pseudopotentials (ref 101).
(103) Mori-Sanchez, P.; Cohen, A. J.; Yang, W. T. *J. Chem. Phys.* **2006**, *125*, 201102.
(104) Ruzsinszky, A.; Perdew, J. P.; Csonka, G. I.; Vydrov, O. A.; Scuseria, G. E. *J. Chem. Phys.* **2007**, *126*, 104102.
(105) Burke, K.; Werschnik, J.; Gross, E. K. U. *J. Chem. Phys.* **2005**, *123*, 062206.
(106) Casida, M. E. In *Recent Advances in Density-Functional Methods part I*; Chong, D. P., Ed.; World Scientific: Singapore, 1995; p 155.
(107) Tretiak, S.; Chernyak, V. *J. Chem. Phys.* **2003**, *119*, 8809−8823.
(108) Neuhauser, D.; Baer, R. *J. Chem. Phys.* **2005**, *123*, 204105.
(109) Kuritz, N.; Stein, T.; Baer, R.; Kronik, L. *J. Chem. Theory Comput.* **2011**, *7*, 2408−2415.
(110) Marques, M.; Rubio, A.; Ullrich, C. A.; Burke, K.; Nogueira, F.; Gross, E. K. U. *Time-Dependent Density Functional Theory*; Springer: Berlin, 2006.
(111) Chelikowsky, J. R.; Kronik, L.; Vasiliev, I. *J. Phys.: Condens. Mater.* **2003**, *15*, R1517−R1547.
(112) Silva-Junior, M. R.; Schreiber, M.; Sauer, S. P. A; Thiel, W. *J. Chem. Phys.* **2008**, *128*, 134110−25.
(113) Adamo, C.; Scuseria, G. E.; Barone, V. *J. Chem. Phys.* **1999**, *111*, 2889−2899.
(114) Furche, F.; Ahlrichs, R. *J. Chem. Phys.* **2002**, *117*, 7433−7447.
(115) Hirata, S.; Head-Gordon, M.; Bartlett, R. J. *J. Chem. Phys.* **1999**, *111*, 10774−10786.
(116) Ziegler, T.; Seth, M.; Krykunov, M.; Autschbach, J.; Wang, F. *THEOCHEM* **2009**, *914*, 106.
(117) Thiele, M.; Gross, E. K. U.; Kümmel, S. *Phys. Rev. Lett.* **2008**, *100*, 153004.
(118) Maitra, N. T. *J. Chem. Phys.* **2005**, *122*, 234104.
(119) Hellgren, M.; Gross, E. K. U. *Phys. Rev. A* **2012**, *85*, 022514.
(120) Autschbach, J. *ChemPhysChem* **2009**, *10*, 1757−1760.
(121) Kaduk, B.; Kowalczyk, T.; Van Voorhis, T. *Chem. Rev.* **2011**, *112*, 321−370.
(122) Yang, Z.-h.; Li, Y.; Ullrich, C. A. ArXiv: 1202.4779v1 2012.
(123) The above failure of the semilocal functional would appear to occur with any multiplicative potential, even the exact Kohn−Sham one. However, this should not be interpreted as a failure of the time-dependent Kohn−Sham equation, which is in principle exact, but only as a failure of the adiabatic linear-response formalism with a nondivergent kernel. For additional perspectives see refs 36, 116−122.
(124) Hanazaki, I. *J. Phys. Chem.* **1972**, *76*, 1982.
(125) Garcia-Lastra, J. M.; Thygesen, K. S. *Phys. Rev. Lett.* **2011**, *106*, 187402.
(126) Blase, X.; Attaccalite, C. *Appl. Phys. Lett.* **2011**, *99*, 171909.
(127) Minami, T.; Nakano, M.; Castet, F. *J. Phys. Chem. Lett.* **2011**, *2*, 1725−1730.
(128) Minami, T.; Ito, S.; Nakano, M. *Int. J. Quantum Chem.* **2012**.
(129) Isaacs, E. B.; Sharifzadeh, S.; Ma, B. W.; Neaton, J. B. *J. Phys. Chem. Lett.* **2011**, *2*, 2531−2537.
(130) Stein, T.; Kronik, L.; Baer, R. *J. Chem. Phys.* **2009**, *131*, 244119−5.
(131) Karolewski, A.; Stein, T.; Baer, R.; Kümmel, S. *J. Chem. Phys.* **2011**, *134*, 151101.
(132) Phillips, H.; Zheng, S.; Hyla, A.; Laine, R.; Goodson, T.; Geva, E.; Dunietz, B. D. *J. Phys. Chem. A* **2011**, *116*, 1137−1145.
(133) Peach, M. J. G.; Benfield, P.; Helgaker, T.; Tozer, D. J. *J. Chem. Phys.* **2008**, *128*, 044118.

(134) Richard, R. M.; Herbert, J. M. *J. Chem. Theory Comput.* **2011**, *7*, 1296−1306.
(135) Wong, B. M.; Hsieh, T. H. *J. Chem. Theory Comput.* **2010**, *6*, 3704−3712.
(136) Lopata, K.; Reslan, R.; Kowaska, M.; Neuhauser, D.; Govind, N.; Kowalski, K. *J. Chem. Theory Comput.* **2011**, *7*, 3686−3693.
(137) Grimme, S.; Parac, M. *ChemPhysChem* **2003**, *4*, 292.
(138) Parac, M.; Grimme, S. *Chem. Phys.* **2003**, *292*, 11−21.
(139) Hieringer, W.; Görling, A. *Chem. Phys. Lett.* **2006**, *419*, 557−562.
(140) Dreuw, A.; Head-Gordon, M. *Chem. Phys. Lett.* **2006**, *426*, 231−233.
(141) Hieringer, W.; Görling, A. *Chem. Phys. Lett.* **2006**, *426*, 234−236.
(142) Phillips, H.; Geva, E.; Dunietz, B. D. To be published.
(143) Sears, J. S.; Körzdörfer, T.; Zhang, C.-R.; Bredas, J.-L. *J. Chem. Phys.* **2011**, *135*, 151103−4.
(144) Peach, M. J. G.; Williamson, M. J.; Tozer, D. J. *J. Chem. Theory Comput.* **2011**, *7*, 3578−3585.
(145) Bylander, D. M.; Kleinman, L. *Phys. Rev. B* **1990**, *41*, 7868−7871.
(146) Gill, P. M. W.; Adamson, R. D.; Pople, J. A. *Mol. Phys.* **1996**, *88*, 1005−1009.
(147) Heyd, J.; Scuseria, G. E.; Ernzerhof, M. *J. Chem. Phys.* **2003**, *118*, 8207−8215.
(148) Krukau, A. V.; Vydrov, O. A.; Izmaylov, A. F.; Scuseria, G. E. *J. Chem. Phys.* **2006**, 125.
(149) Adamo, C.; Barone, V. *J. Chem. Phys.* **1999**, *110*, 6158−6170.
(150) Ernzerhof, M.; Scuseria, G. E. *J. Chem. Phys.* **1999**, *110*, 5029−5036.
(151) Janesko, B. G.; Henderson, T. M.; Scuseria, G. E. *Phys. Chem. Chem. Phys.* **2009**, *11*, 443−454.
(152) Paier, J.; Marsman, M.; Hummer, K.; Kresse, G.; Gerber, I. C.; Angyan, J. G. *J. Chem. Phys.* **2006**, *124*, 154709.
(153) Brothers, E. N.; Izmaylov, A. F.; Normand, J. O.; Barone, V.; Scuseria, G. E. *J. Chem. Phys.* **2008**, *129*, 011102.
(154) Zhao, Y.; Truhlar, D. G. *Acc. Chem. Res.* **2008**, *41*, 157−167.
(155) Zhao, Y.; Truhlar, D. G. *Theor. Chem. Acc.* **2008**, *120*, 215−241.
(156) Zhao, Y.; Truhlar, D. G. *J. Phys. Chem. A* **2006**, *110*, 13126−13130.
(157) Vydrov, O. A.; Heyd, J.; Krukau, A. V.; Scuseria, G. E. *J. Chem. Phys.* **2006**, *125*, 074106.
(158) Biller, A.; Tamblyn, I.; Neaton, J. B.; Kronik, L. *J. Chem. Phys.* **2011**, *135*, 164706−6.
(159) Marom, N.; Hod, O.; Scuseria, G. E.; Kronik, L. *J. Chem. Phys.* **2008**, *128*, 164107.
(160) Barone, V.; Peralta, J. E.; Wert, M.; Heyd, J.; Scuseria, G. E. *Nano Lett.* **2005**, *5*, 1621−1624.
(161) Barone, V.; Hod, O.; Peralta, J. E.; Scuseria, G. E. *Acc. Chem. Res.* **2011**, *44*, 269−279.
(162) Bisti, F.; Stroppa, A.; Donarelli, M.; Picozzi, S.; Ottaviano, L. *Phys. Rev. B* **2011**, *84*, 195112.
(163) Sai, N.; Barbara, P. F.; Leung, K. *Phys. Rev. Lett.* **2011**, *106*, 226403.
(164) Imamura, Y.; Kobayashi, R.; Nakai, H. *Chem. Phys. Lett.* **2011**, *513*, 130−135.
(165) Marom, N.; Tkatchenko, A.; Scheffler, M.; Kronik, L. *J. Chem. Theory Comput.* **2010**, *6*, 81−90.
(166) Körzdörfer, T.; Kümmel, S. *Phys. Rev. B* **2010**, *82*, 155206.
(167) Tawada, Y.; Tsuneda, T.; Yanagisawa, S.; Yanai, T.; Hirao, K. *J. Chem. Phys.* **2004**, *120*, 8425−8433.
(168) Lange, A. W.; Rohrdanz, M. A.; Herbert, J. M. *J. Phys. Chem. B* **2008**, *112*, 6304−6308.
(169) Wong, B. M.; Piacenza, M.; Della Sala, F. *Phys. Chem. Chem. Phys.* **2009**, *11*, 4498−4508.
(170) Akinaga, Y.; Ten-No, S. *Int. J. Quantum Chem.* **2009**, *109*, 1905−1914.
(171) Peach, M. J. G.; Le Sueur, C. R.; Ruud, K.; Guillaume, M.; Tozer, D. J. *Phys. Chem. Chem. Phys.* **2009**, *11*, 4465−4470.
(172) Mohammed, A.; Agren, H.; Norman, P. *Phys. Chem. Chem. Phys.* **2009**, *11*, 4539−4548.
(173) Andzelm, J.; Rinderspacher, B. C.; Rawlett, A.; Dougherty, J.; Baer, R.; Govind, N. *J. Chem. Theory Comput.* **2009**, *5*, 2835−2846.
(174) Perdew, J. P.; Schmidt, K. Jacob's Ladder of Density Functional Approximations for the Exchange-Correlation Energy. In *Density functional theory and its application to materials*; Antwerp, Belgium, June 8−10, 2000; Van Doren, V. E., Van Alsenoy, C., Geerlings, P., Eds.; American Institute of Physics: Melville, NY, 2001.
(175) Stein, T.; Kronik, L.; Baer, R. To be published.
(176) B3LYP and BNL results were taken from ref 88, and PBE results were obtained using the same method. GW results were taken from ref 126. For PTCDA, similar HOMO−LUMO gaps was reported in refs 177 and 178. For $H_2$TPP, a somewhat smaller fundamental gap was obtained from GW in ref 179, possibly due to the "one-shot" (G0W0) nature of their calculation. GW-BSE optical excitation energies were taken from ref 180 for $H_2$TPP and from ref 178 for PTCDA. For $H_2$TPP, the experimental ionization potential and electron affinity were taken from refs 179 and 181, respectively. For PTCDA, the experimental ionization potential was taken from ref 177. Experimental optical gaps for $H_2$TPP and PTCDA were taken from refs 182 and 183, respectively. Note that for $H_2$TPP, some uncertainty in the assignment of optical gap due to the identification of vibrational contributions may arise. (compare, e.g., our assignment to that of ref 180). However, the difference is small (0.2 eV) and therefore of no special consequence for either this work or the work of ref 180.
(177) Dori, N.; Menon, M.; Kilian, L.; Sokolowski, M.; Kronik, L.; Umbach, E. *Phys. Rev. B* **2006**, *73*, 195208.
(178) Sharifzadeh, S.; Biller, A.; Kronik, L.; Neaton, J. B. *Phys. Rev. B* **2012**, *85*, 125307.
(179) Stenuit, G.; Castellarin-Cudia, C.; Plekan, O.; Feyer, V.; Prince, K. C.; Goldoni, A.; Umari, P. *Phys. Chem. Chem. Phys.* **2010**, *12*, 10812−10817.
(180) Palummo, M.; Hogan, C.; Sottile, F.; Bagala, P.; Rubio, A. *J. Chem. Phys.* **2009**, *131*, 084102.
(181) Chen, H. L.; Pan, Y. H.; Groh, S.; Hagan, T. E.; Ridge, D. P. *J. Am. Chem. Soc.* **1991**, *113*, 2766−2767.
(182) Edwards, L.; Dolphin, D. H.; Gouterma., M; Adler, A. D. *J. Mol. Spectrosc.* **1971**, *38*, 16.
(183) Wewer, M.; Stienkemeier, F. *J. Chem. Phys.* **2004**, *120*, 1239−1244.